

Split-Session Cluster GARCH for Overnight and Intraday Returns: The Role of Tail Heterogeneity

Xinxian Chen[‡] Peter Reinhard Hansen^{§*} Chen Tong[‡]

[‡]Department of Finance, School of Economics, Xiamen University, China

[§]Department of Economics, University of North Carolina at Chapel Hill, United States

July 7, 2026

Abstract

We propose the Split-Session Cluster GARCH model for heavy-tailed multivariate dependence among asset returns decomposed into overnight and intraday components. The model uses convolution- t distributions to allow tail behavior to differ across clusters defined by trading sessions and, within each session, by economic sectors. It also accommodates block-structured conditional correlation matrices, preserving parsimony and scalability in high-dimensional settings. The resulting likelihood remains tractable and yields a score-driven specification for dynamic correlations. We apply the model to U.S. equity returns in six-asset and 100-asset applications. The results reveal pronounced tail heterogeneity between overnight and intraday returns. Model comparisons show that session-specific tail parameters substantially improve fit relative to a common multivariate- t specification, while sector-level tail partitioning delivers additional gains concentrated mainly in the overnight component. In the 100-asset application, asset-level tail heterogeneity delivers the strongest out-of-sample likelihood and global minimum-variance (GMV) portfolio performance.

Keywords: Multivariate GARCH; Overnight returns; Tail heterogeneity; Block correlation structure; High-dimensional dependence; Score-driven models.

*Corresponding author: Peter Reinhard Hansen (hansen@unc.edu). Chen Tong acknowledges financial support from the Youth Fund of the National Natural Science Foundation of China (72301227) and the Fujian Provincial Natural Science Foundation of China (2025J08008).

1 Introduction

Understanding dependence among financial asset returns is central to portfolio allocation, risk management, and asset pricing. A large literature models conditional covariance matrices by separating volatility and correlation dynamics, as in the CCC model of [Bollerslev \(1990\)](#) and the DCC model of [Engle \(2002\)](#); see also [Tse and Tsui \(2002\)](#), [Aielli \(2013\)](#), and [Engle, Ledoit, and Wolf \(2019\)](#). Recent studies further develop dynamic covariance and correlation forecasts for equity markets, portfolio selection, and systemic-risk measurement ([Symitsi, Symeonidis, Kourtis, and Markellos, 2018](#); [Moura, Santos, and Ruiz, 2020](#); [De Nard, Engle, Ledoit, and Wolf, 2022](#); [Honig and Kircher, 2025](#); [Girardi and Ergün, 2013](#)). Despite these advances, dynamic correlation modeling remains challenging because the number of correlations grows quadratically with the number of assets, positive definiteness must be preserved, and cross-product-based updates can be sensitive to extremes. These issues are amplified in heavy-tailed multivariate systems, where misspecified tail behavior can distort dynamic dependence updates.

To address these challenges, a growing literature imposes structured representations on large correlation systems. One strand restricts correlation dynamics through factor structures (e.g., [Creal and Tsay, 2015](#); [Oh and Patton, 2023](#)), while another uses block correlation matrices (e.g., [Engle and Kelly, 2012](#); [Tong, Hansen, and Archakov, 2026](#); [Archakov, Hansen, and Lunde, 2026](#)) or combines factor and block structures ([Tong and Hansen, 2026](#)). In parallel, the correlation parameterization of [Archakov and Hansen \(2021\)](#) maps unconstrained real-valued parameters into positive definite correlation matrices. Separately, the canonical block representation of [Archakov and Hansen \(2024\)](#) exploits block structure to reduce the dimension of the correlation system from the asset-pair level to the block-pair level. The score-driven framework of [Creal, Koopman, and Lucas \(2013\)](#) provides a likelihood-based method for updating time-varying parameters in dynamic dependence models.

Most multivariate volatility and correlation studies use daily close-to-close returns, although these returns combine overnight close-to-open and intraday open-to-close components with distinct information-arrival mechanisms. During trading hours, prices adjust continuously through trading, whereas overnight information accumulates and is incorporated when the market reopens. Consistent with this distinction, [French and Roll \(1986\)](#) and [Lockwood and McInish \(1990\)](#) document sharp

differences between trading and non-trading returns, while [Moshirian, Nguyen, and Pham \(2012\)](#), [Barclay and Hendershott \(2003\)](#), and [Lou, Polk, and Skouras \(2019\)](#) show that overnight information, after-hours trading, and heterogeneous investor clienteles affect price discovery and return dynamics. These findings suggest that treating daily returns as homogeneous close-to-close objects may obscure important session-level differences in distributions and cross-asset dependence.

A more recent literature explicitly models overnight and intraday returns separately. [Blanc, Chicheportiche, and Bouchaud \(2014\)](#) document important differences in the volatility dynamics of the two trading sessions. [Linton and Wu \(2020\)](#) propose a semiparametric coupled component DCS-EGARCH model for intraday and overnight volatility. [Dhaene and Wu \(2020\)](#) develop mixed-frequency multivariate GARCH models that combine high-frequency intraday returns and overnight returns to forecast lower-frequency covariance matrices. [Kang and Babbs \(2012\)](#) introduce a multivariate copula-GARCH model for overnight and intraday returns with DCC-type dependence. Relatedly, based on high-frequency intraday data, [Kim, Shin, and Wang \(2023\)](#) propose a univariate overnight GARCH-Itô model with separate open-to-close and close-to-open volatility processes, and [Kim, Oh, Song, and Wang \(2024\)](#) extend this idea to large volatility matrix estimation and prediction in a high-dimensional factor framework.

While these studies provide important insights into session-level volatility and dependence modeling, several rely on high-frequency intraday data or realized measures. By contrast, we model the dynamic correlation structure of multivariate overnight and intraday return innovations using only daily open and close prices, which are widely available across assets and markets. More importantly, existing cross-asset correlation models often pool overnight and intraday components and typically impose a common tail structure across assets or broad asset groups. Such restrictions are problematic when tail behavior differs across both trading sessions and economically meaningful groups such as sectors. A flexible multivariate heavy-tailed model should therefore allow tail heterogeneity across both time and cross-sectional dimensions while preserving a tractable and positive definite dynamic correlation structure.

In this paper, we develop the Split-Session Cluster GARCH model for heavy-tailed multivariate dependence among overnight and intraday return innovations. The model extends the Cluster GARCH

framework of [Tong et al. \(2026\)](#), which was based on daily close-to-close returns, to a setting in which overnight and intraday returns are modeled as distinct but related components. The term “Split-Session” reflects the decomposition of daily returns into overnight and intraday components, while “Cluster” refers to the partitioning of innovations into economically meaningful groups, such as trading sessions and sectors, each with its own tail parameter under the convolution- t distribution of [Hansen and Tong \(2026\)](#). The proposed framework combines this clustered tail specification with the unconstrained correlation parameterization of [Archakov and Hansen \(2021\)](#), ensuring positive definiteness of the dynamic correlation matrix. To improve scalability, we further introduce block correlation structures for the overnight and intraday correlation matrices and use their canonical representation ([Archakov and Hansen, 2024](#)).

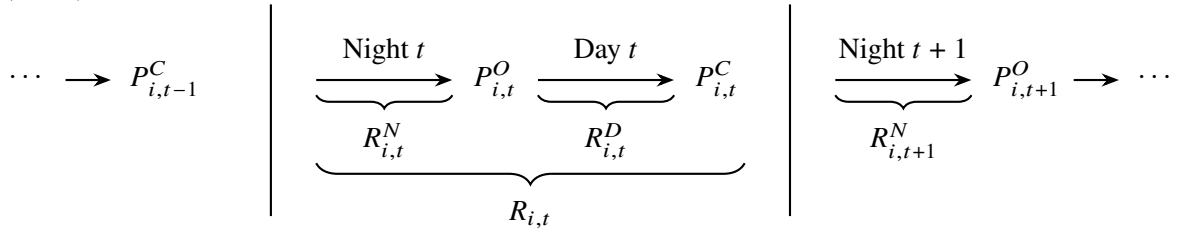
This paper makes four main contributions. First, we extend the overnight–intraday return literature from volatility modeling to dynamic multivariate dependence modeling. Our approach explicitly models the conditional correlation matrices of standardized overnight and intraday innovations and allows correlation updates to differ across trading sessions. Second, we use the convolution- t distributional framework of [Hansen and Tong \(2026\)](#) to study session- and group-specific tail heterogeneity in a dynamic correlation setting. In our application, clusters are defined by trading sessions and, within each session, by economic groups such as sectors. This allows the model to distinguish between common-tail multivariate- t specifications, session-specific tail specifications, sector-level tail partitions, and fully asset-specific Hetero- t specifications. The empirical results show that tail heterogeneity is not merely a marginal distributional feature: the distinction between overnight and intraday tails materially affects score-driven correlation updating and model fit. Third, we provide a scalable implementation of the split-session dependence model by combining score-driven correlation dynamics with the canonical block-correlation representation. This yields a scalable dependence model in which correlation dynamics are updated at the block-pair rather than asset-pair level, reducing dimensionality while preserving positive definiteness. Fourth, we provide empirical evidence from both a six-asset application and a 100-asset application. The six-asset application, based on 20 years of daily stock returns for representative U.S. equities from two industrial sectors, allows us to examine the mechanisms of session-level and sector-level tail heterogeneity in detail. The 100-asset application shows that the block specification

remains tractable in larger cross sections and that the Hetero- t model performs best, suggesting that asset-level tail heterogeneity becomes more valuable as the dimension grows. We further assess the economic relevance of the high-dimensional forecasts using global minimum variance (GMV) portfolio performance.

The paper proceeds as follows. Section 2 introduces the asset-level Coupled EGARCH model for overnight and intraday volatility. Section 3 presents the dynamic correlation matrix framework. Section 4 introduces the multivariate- t , Gaussian, Cluster- t , and Hetero- t specifications as special cases of the convolution- t framework. Section 5 derives the corresponding scores and Fisher information matrices, including the canonical block representation. Section 6 introduces the DCC benchmark model. Section 7 presents the six-asset empirical application, while Section 8 examines the 100-asset high-dimensional application. Section 9 concludes.

2 The Coupled EGARCH Model

We decompose the daily close-to-close return of asset i on day t , $R_{i,t}$, into an overnight return, $R_{i,t}^N$, and an intraday return, $R_{i,t}^D$, where $R_{i,t}^N = \log(P_{i,t}^O/P_{i,t-1}^C)$ and $R_{i,t}^D = \log(P_{i,t}^C/P_{i,t}^O)$. Following [Linton and Wu \(2020\)](#), the timeline is:



To capture the sequential nature of information within a trading day, we define two nested information sets for asset i : $\mathcal{F}_{i,t}^N = \sigma(\{R_{i,\tau}^N, R_{i,\tau}^D\}_{\tau \leq t-1})$ and $\mathcal{F}_{i,t}^D = \sigma(\mathcal{F}_{i,t}^N \cup \{R_{i,t}^N\})$. Here, $\mathcal{F}_{i,t}^N$ contains all past overnight and intraday returns available at the close of day $t-1$, while $\mathcal{F}_{i,t}^D$ augments $\mathcal{F}_{i,t}^N$ by incorporating newly realized overnight return on day t .

We model the joint dynamics of overnight and intraday returns using a vector autoregressive (VAR)

framework. The conditional mean is given by:

$$\begin{pmatrix} 1 & 0 \\ -\delta_i & 1 \end{pmatrix} \begin{pmatrix} R_{i,t}^N \\ R_{i,t}^D \end{pmatrix} = \begin{pmatrix} \mu_i^N \\ \mu_i^D \end{pmatrix} + \begin{pmatrix} \phi_{11,i} & \phi_{12,i} \\ \phi_{21,i} & \phi_{22,i} \end{pmatrix} \begin{pmatrix} R_{i,t-1}^N \\ R_{i,t-1}^D \end{pmatrix} + \begin{pmatrix} \sqrt{h_{i,t}^N} & 0 \\ 0 & \sqrt{h_{i,t}^D} \end{pmatrix} \begin{pmatrix} Z_{i,t}^N \\ Z_{i,t}^D \end{pmatrix}, \quad (1)$$

where $h_{i,t}^N = \text{var}(R_{i,t}^N | \mathcal{F}_{i,t}^N)$ and $h_{i,t}^D = \text{var}(R_{i,t}^D | \mathcal{F}_{i,t}^D)$ denote the conditional variances. The terms $Z_{i,t}^N$ and $Z_{i,t}^D$ are the standardized innovations with zero mean and unit variance.

Regarding the mean dynamics, the parameter δ_i captures the contemporaneous impact of the overnight return on the intraday return within the same trading day. Due to the triangular structure of the system, the intraday return $R_{i,t}^D$ depends on the term $\delta_i R_{i,t}^N$. As a result, a positive δ_i implies an overnight-intraday continuation, whereas a negative δ_i indicates reversal. The vector $(\mu_i^N, \mu_i^D)'$ contains the intercepts of the two return components. The matrix $\Phi_i = \begin{pmatrix} \phi_{11,i} & \phi_{12,i} \\ \phi_{21,i} & \phi_{22,i} \end{pmatrix}$ captures both own-lag and cross-lag dependence in returns for asset i , allowing past overnight and intraday returns to influence current returns across trading sessions.

To capture asymmetric leverage effects and bidirectional volatility spillovers between the overnight and intraday sessions, we model the conditional log-variances using a Coupled Exponential GARCH (Coupled EGARCH) specification. It is given by:

$$\begin{aligned} \log h_{i,t}^N &= \omega_i^N + \beta_i^N \log h_{i,t-1}^N + \tau_{1,i}^N Z_{i,t-1}^N + \tau_{2,i}^N |Z_{i,t-1}^N| + \underbrace{\delta_{1,i}^N Z_{i,t-1}^D + \delta_{2,i}^N |Z_{i,t-1}^D|}_{\text{spillover from previous day}}, \\ \log h_{i,t}^D &= \omega_i^D + \beta_i^D \log h_{i,t-1}^D + \tau_{1,i}^D Z_{i,t-1}^D + \tau_{2,i}^D |Z_{i,t-1}^D| + \underbrace{\delta_{1,i}^D Z_{i,t}^N + \delta_{2,i}^D |Z_{i,t}^N|}_{\text{spillover from current night}}. \end{aligned}$$

The EGARCH specification ensures positivity of conditional variances without parameter restrictions and accommodates asymmetric responses to positive and negative shocks. The intercepts ω_i^N and ω_i^D , together with the persistence parameters and average shock-magnitude terms, determine the baseline levels of overnight and intraday log-volatility, respectively. The parameters β_i^N and β_i^D measure the persistence in overnight and intraday volatility. The coefficients $\tau_{1,i}^c$ capture the sign effects, while $\tau_{2,i}^c$ capture the magnitude effects, for $c \in \{N, D\}$. This structure allows volatility to respond asymmetrically to positive and negative return innovations, reflecting the leverage effect commonly observed in equity

markets. The parameters $\delta_{1,i}^N, \delta_{2,i}^N, \delta_{1,i}^D, \delta_{2,i}^D$ capture volatility spillovers between overnight and intraday periods. Specifically, $\delta_{1,i}^N$ and $\delta_{2,i}^N$ measure the impact of intraday shocks from day $t - 1$ on overnight volatility, while $\delta_{1,i}^D$ and $\delta_{2,i}^D$ capture the effect of overnight shocks on intraday volatility within the same trading day.

We estimate the model asset by asset using quasi-maximum likelihood estimation (QMLE) under the Gaussian assumption. The remaining distributional features of the standardized innovations, including heavy tails and tail heterogeneity across sessions, are modeled in the second-stage correlation model. The resulting standardized innovations, $Z_{i,t}^N$ and $Z_{i,t}^D$, serve as the inputs to the multivariate correlation model introduced in the next section, where their joint distribution and their cross-asset dependence structure are modeled explicitly. The second-stage likelihood treats the first-stage standardized innovations as given, so the reported second-stage standard errors are conditional on the first-stage filtering step.

3 The Dynamic Correlation Matrix Modeling Framework

Let $Z_t = (Z_t^N, Z_t^D)'$ denote the $2n \times 1$ vector of standardized innovations for all n assets, where Z_t^N and Z_t^D are the $n \times 1$ vectors of overnight and intraday innovations, respectively. Building on the asset-specific filtrations in Section 2, define $\mathcal{F}_t = \sigma(\{R_\tau^N, R_\tau^D\}_{\tau \leq t-1})$ as the information available at the beginning of day t , and $\mathcal{G}_t = \sigma(\mathcal{F}_t \cup \{R_t^N\})$ as the augmented filtration that incorporates the realized overnight returns prior to the intraday session.

In the most general setting, the joint conditional correlation matrix of the $2n \times 1$ innovation vector Z_t can be partitioned into a full block structure:

$$C_t = \begin{pmatrix} C_t^N & C_t^{ND} \\ C_t^{DN} & C_t^D \end{pmatrix} \in \mathbb{R}^{2n \times 2n},$$

where C_t^N and C_t^D are the overnight and intraday correlation matrices, and $C_t^{ND} = (C_t^{DN})'$ captures cross-session dependence. Details of the likelihood construction and related derivations under this general specification are provided in Appendix C.

The first-stage Coupled EGARCH model removes the most direct same-asset overnight-intraday

dependence through the contemporaneous transmission parameter δ_i in the mean equation and the cross-session volatility spillovers. We then impose $C_t^{ND} = \mathbf{0}$ as a parsimonious block-diagonal specification for the standardized innovations. This restriction is broadly consistent with the residual cross-session correlation diagnostics reported in Appendix B, where the remaining within-asset and cross-asset cross-session correlations are small in magnitude and far below the within-session correlations.

Because the trading day unfolds sequentially, the augmented filtration \mathcal{G}_t is useful for describing the information available before the intraday session. Under joint specifications such as the common multivariate- t distribution, the conditional distribution of Z_t^D may also depend on the realized overnight shocks Z_t^N . In the block-diagonal session-specific specifications developed below, this dependence is restricted through the assumed separation between overnight and intraday innovation blocks. Accordingly, the conditional correlation matrix simplifies to $C_t = \text{blockdiag}(C_t^N, C_t^D) \in \mathbb{R}^{2n \times 2n}$.

Definition 1 (Block Correlation Matrix). $C \in \mathbb{R}^{n \times n}$ is a block matrix with K blocks, if it is expressed as

$$C = \begin{bmatrix} C_{[1,1]} & C_{[1,2]} & \cdots & C_{[1,K]} \\ C_{[2,1]} & C_{[2,2]} & & \\ \vdots & & \ddots & \\ C_{[K,1]} & & & C_{[K,K]} \end{bmatrix}, \quad \text{where } C_{[k,k]} = \begin{bmatrix} 1 & \rho_{kk} & \cdots & \rho_{kk} \\ \rho_{kk} & 1 & \ddots & \\ \vdots & \ddots & \ddots & \\ \rho_{kk} & & & 1 \end{bmatrix}, \quad C_{[k,l]} = \begin{bmatrix} \rho_{kl} & \cdots & \rho_{kl} \\ \vdots & \ddots & \\ \rho_{kl} & & \rho_{kl} \end{bmatrix}$$

for $k \neq l$, and $\sum_{k=1}^K n_k = n$ with $n_k \geq 1$.

3.1 The Unrestricted Parametrization of (Block) Correlation Matrix

We model the overnight and intraday correlation matrices using the score-driven framework by [Creal et al. \(2013\)](#). Following [Archakov and Hansen \(2021\)](#), we parameterize each block of the conditional correlation matrix via the matrix logarithm transformation. Let $\gamma_t^N = \text{vecl}(\log C_t^N) \in \mathbb{R}^d$ and $\gamma_t^D = \text{vecl}(\log C_t^D) \in \mathbb{R}^d$, where $d = n(n-1)/2$ and $\text{vecl}(\cdot)$ selects and vectorizes the strictly lower triangular elements of the matrix. This transformation provides an unconstrained parameterization of the correlation matrices and guarantees C_t remains a unique positive definite correlation matrix.

Importantly, the matrix logarithm preserves block structures, as illustrated below

$$\gamma(C) \equiv \text{vecl} \left[\log \begin{pmatrix} 1.0 & 0.6 & 0.2 & 0.2 \\ 0.6 & 1.0 & 0.2 & 0.2 \\ 0.2 & 0.2 & 1.0 & 0.4 \\ 0.2 & 0.2 & 0.4 & 1.0 \end{pmatrix} \right] = \text{vecl} \begin{pmatrix} -0.24 & 0.676 & 0.137 & 0.137 \\ 0.676 & -0.24 & 0.137 & 0.137 \\ 0.137 & 0.137 & -0.11 & 0.404 \\ 0.137 & 0.137 & 0.404 & -0.11 \end{pmatrix} = \begin{pmatrix} 0.676 \\ 0.137 \times \iota_4 \\ 0.404 \end{pmatrix},$$

where ι_n is an $n \times 1$ vector of ones, and C can be C_t^N or C_t^D .

For a block matrix with K blocks as defined in Definition 1, $\gamma(C)$ will have at most $(K + 1)K/2$ distinct elements, such that we can write $\gamma = B\eta$, where B is a known zero-one selector matrix and η is a subvector of γ . In the example above we have, $\gamma = B\eta$, $B = \text{blockdiag}(1, \iota_4, 1) \in \mathbb{R}^{6 \times 3}$, and $\eta = (0.676, 0.137, 0.404)'$. Parameterizing the block correlation matrix, C , with η does not impose additional superfluous restrictions, see [Tong and Hansen \(2023\)](#). Thus, any nonsingular block correlation matrix corresponds to a unique η vector, and any dynamic block correlation model can be expressed as a dynamic model for η .

3.2 The Score-driven Framework for Dynamic (Block) Correlation Matrix

In the general case without imposing block structure, we can stack the parameters into a joint vector $\gamma_t = (\gamma_t^{N'}, \gamma_t^{D'})' \in \mathbb{R}^{n(n-1)}$, and then model the dynamics of γ_t via the score-driven framework of [Creal et al. \(2013\)](#) with a vector autoregressive model of order one, VAR(1):

$$\gamma_{t+1} = (I_{n(n-1)} - \beta) \mu + \beta \gamma_t + \alpha S_t^{-1} \nabla_t, \quad (2)$$

where μ is the unconditional mean of γ_t , and α and β are $n(n-1) \times n(n-1)$ diagonal matrices. The vector ∇_t is the score of the joint log-likelihood, ℓ_t , taken with respect to γ_t :

$$\nabla_t = \frac{\partial \ell_t}{\partial \gamma_t} = \left(\frac{\partial \ell_t}{\partial \gamma_t^{N'}}, \frac{\partial \ell_t}{\partial \gamma_t^{D'}} \right)' \equiv \left(\nabla_t^{N'}, \nabla_t^{D'} \right)'. \quad (3)$$

The scaling matrix S_t is set to the conditional Fisher information matrix, $S_t = \mathbb{E}_{t-1} [\nabla_t \nabla_t']$, following [Creal et al. \(2013\)](#). This choice makes the scaled score $S_t^{-1} \nabla_t$ an approximate Newton step in the

parameter space, ensuring that the magnitude of correlation updates is automatically adjusted for the local curvature of the likelihood surface. To reduce computational cost, we use a diagonal approximation of S_t^{-1} , whereby each parameter is scaled by its own marginal Fisher information.

When a sector-based block structure is imposed on C_t^N and C_t^D , the dimension of γ_t^N and γ_t^D is reduced from $n(n-1)/2$ to $K(K+1)/2$. From $\gamma_t^N = B^N \eta_t^N$ and $\gamma_t^D = B^D \eta_t^D$, we can stack them into a joint condensed vector $\eta_t = (\eta_t^{N'}, \eta_t^{D'})' \in \mathbb{R}^{K(K+1)}$, the score-driven dynamics for the condensed parameters become:

$$\eta_{t+1} = (I_{K(K+1)} - \beta) \mu + \beta \eta_t + \alpha S_{\eta,t}^{-1} \nabla_{\eta,t}, \quad (4)$$

Combined with the canonical representation in Subsection 5.4, the block structure allows the score and information matrices to be evaluated in a lower-dimensional system governed by the number of blocks K rather than the number of assets n , which is desirable in high-dimensional settings.

The form of the score and Fisher information matrix depends on the distributional specifications introduced below.

4 Multivariate Convolution- t Distributions for Clustered Tail Heterogeneity

This section introduces the distributional component of the model. The convolution- t framework of [Hansen and Tong \(2026\)](#) provides a tractable class of multivariate heavy-tailed distributions in which different subsets of variables may have different degrees of freedom. It nests the multivariate- t as a special case. Flexible non-Gaussian specifications are particularly relevant in financial covariance modeling, where departures from elliptical return distributions can affect dependence modeling and portfolio decisions; see, for example, [Paolella, Polak, and Walker \(2021\)](#). Our focus differs by using clustered convolution- t distributions to model session- and group-specific tail heterogeneity in dynamic correlation systems.

A convolution- t random vector is constructed by applying a correlation transformation to several mutually independent multivariate t -distributed components. Let $C_t^{1/2}$ denote the symmetric positive

definite square root of C_t , and write

$$Z_t = C_t^{1/2} U_t, \quad \text{where } U_t = (U'_{1,t}, \dots, U'_{G,t})', \quad U_{g,t} \stackrel{\text{ind}}{\sim} t_{\nu_g}^{\text{std}}(0, I_{m_g}),$$

where $\nu_g > 2$ and $\sum_{g=1}^G m_g = 2n$. Each cluster carries its own degrees-of-freedom parameter ν_g , so that tail thickness can vary across groups of variables while the likelihood remains analytically tractable.

The cluster partition can be chosen to reflect economic structure. At one extreme, all variables share a single cluster ($G = 1$), which collapses to the standard multivariate- t . At the other extreme, each asset in each session forms its own cluster ($G = 2n, m_g = 1$), giving every variable its own tail parameter. In our setting, the most natural partition groups variables by trading session, yielding $G = 2$ clusters, which means one for overnight innovations and one for intraday innovations, each with its own degrees-of-freedom, ν_N and ν_D .

More generally, the convolution- t framework allows further flexible partitioning. Assets within the overnight and intraday sessions could be grouped into multiple clusters, each associated with its own tail parameter. For instance, assets could be grouped by economic industry sectors, allowing tail behavior to vary across both sessions and economic sectors simultaneously. Figure 1 illustrates this structure: daily returns are first decomposed into overnight and intraday components, and each session is then partitioned into K sector-based clusters, with each cluster carrying its own degrees-of-freedom parameter $\nu_{k,c}$, for $k = 1, \dots, K$ and $c \in \{N, D\}$. The total number of clusters is thus $G = 2K$. We consider all of these specifications in the empirical analysis.

Since the clusters $U_{g,t}$ are mutually independent, the joint log-likelihood is additively separable:

$$\ell_t(Z_t | \mathcal{F}_t) = -\frac{1}{2} \log |C_t| + \sum_{g=1}^G \ell_{g,t}(U_{g,t}; \nu_g), \quad (5)$$

where $\ell_{g,t}$ denotes the log-density contribution of the g -th cluster.

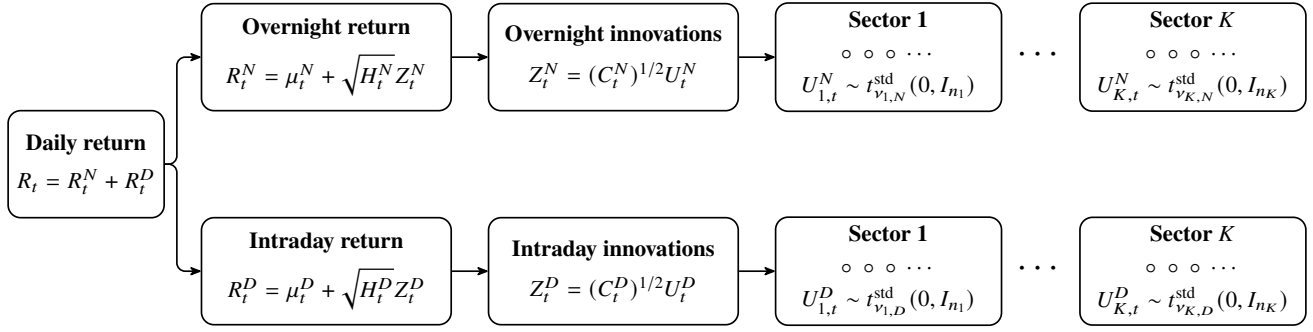


Figure 1: Return Decomposition and Sessions/Sectoral Clustering

4.1 Case 1: Multivariate t -Distribution (MT)

Under the standardized multivariate- t distribution, $Z_t | \mathcal{F}_t \sim t_{2n,\nu}^{\text{std}}(0, C_t)$, with log-likelihood given by

$$\ell_t(Z_t | \mathcal{F}_t) = c_{\nu,2n} - \frac{1}{2} \log |C_t| - \frac{\nu + 2n}{2} \log \left(1 + \frac{1}{\nu - 2} Z_t' C_t^{-1} Z_t \right), \quad (6)$$

where $c_{\nu,2n}$ is the normalizing constant, and the scaling by $\nu - 2$ ensures that the distribution has unit variance for $\nu > 2$. The Gaussian specification is nested as the limiting case $\nu \rightarrow \infty$, under which the tail adjustment disappears and the multivariate- t likelihood reduces to the Gaussian likelihood.

Because all $2n$ elements share a common degrees-of-freedom parameter ν , the multivariate- t specification imposes a homogeneous tail structure across overnight and intraday innovations.

By the marginal-conditional representation of the standardized multivariate- t distribution,

$$Z_t^N | \mathcal{F}_t \sim t_{\nu}^{\text{std}}(0, C_t^N), \quad Z_t^D | \mathcal{G}_t \stackrel{d}{=} Z_t^D | Z_t^N \sim t_{\nu+n}^{\text{std}} \left(C_t^{DN} (C_t^N)^{-1} Z_t^N, \tilde{C}_t^D \right),$$

where

$$\tilde{C}_t^D = \frac{\nu - 2 + q_N}{\nu + n - 2} \left(C_t^D - C_t^{DN} (C_t^N)^{-1} C_t^{ND} \right), \quad q_N = (Z_t^N)' (C_t^N)^{-1} Z_t^N.$$

This implies the decomposition $\ell_t = \ell(Z_t^N | \mathcal{F}_t) + \ell(Z_t^D | \mathcal{G}_t)$. However, the two components remain jointly governed by the same degrees-of-freedom parameter ν , and the conditional distribution of Z_t^D depends on Z_t^N . Thus, the model imposes a homogeneous tail structure across sessions.

Under the block-diagonal specification $C_t^{ND} = \mathbf{0}$, this reduces to

$$Z_t^D | \mathcal{G}_t \sim t_{\nu+n}^{\text{std}} \left(0, \frac{\nu - 2 + q_N}{\nu + n - 2} C_t^D \right), \quad q_N = (Z_t^N)' (C_t^N)^{-1} Z_t^N.$$

Thus, even when $C_t^{ND} = \mathbf{0}$, the conditional intraday distribution is scaled by the realized overnight shock and both sessions remain governed by the same tail parameter. This motivates the convolution- t specifications below, which allow tail behavior to differ across sessions while preserving tractability.

4.2 Case 2: Cluster- t Distributions

The Cluster- t specification arises when G is determined by a predefined grouping structure. In this case, each subvector $U_{g,t}$ follows a multivariate t -distribution, and variables within the same cluster share a common degrees-of-freedom parameter ν_g . Aggregating the cluster-specific contributions gives

$$\ell_t(Z_t | \mathcal{F}_t) = -\frac{1}{2} \log |C_t| + \sum_{g=1}^G \left[c_{\nu_g, m_g} - \frac{\nu_g + m_g}{2} \log \left(1 + \frac{U'_{g,t} U_{g,t}}{\nu_g - 2} \right) \right], \quad (7)$$

where c_{ν_g, m_g} is the normalizing constant for the g -th cluster.

One important feature of the Cluster- t specification is that it preserves the nonlinear dependence among variables within each cluster. Because variables in the same cluster share a common tail thickness, the model can capture common extreme realizations within a sector or within a trading session.

4.3 Case 3: Hetero- t Distributions

The Hetero- t is the special case in which each element of the innovation vector forms its own cluster, so that $G = 2n$ and $m_g = 1$. This specification allows each variable to have its own degrees-of-freedom, providing the most flexible specification for heterogeneous tail behavior. Under this limiting case, every asset j in each session c carries a unique parameter $\nu_{j,c}$, resulting in $G = 2n$ independent univariate clusters. Thus, the log-likelihood is given by

$$\ell_t(Z_t | \mathcal{F}_t) = -\frac{1}{2} \log |C_t| + \sum_{g=1}^{2n} \left[c_{\nu_g, 1} - \frac{\nu_g + 1}{2} \log \left(1 + \frac{1}{\nu_g - 2} U_{g,t}^2 \right) \right], \quad (8)$$

where $c_{\nu_g, 1}$ is the normalizing constant, and $U_{g,t}$ is the g -th element of the standardized vector U_t . However, this flexibility comes at a cost. When $m_g = 1$, the components of U_t are mutually independent, implying that no joint tail dependence is preserved prior to the correlation transformation. As a result, the Hetero- t specification captures marginal heavy tails but does not preserve a shared cluster-level tail

component before the correlation transformation. It therefore provides a less direct representation of clustered extreme co-movements than the Cluster- t specification.

The choice between Cluster- t and Hetero- t therefore reflects a trade-off: the former preserves within-group tail dependence while allowing for moderate heterogeneity, whereas the latter maximizes marginal flexibility at the expense of weakening the cluster-level tail structure. Thus, the convolution- t framework provides a continuum of heavy-tailed multivariate specifications, ranging from a common-tail elliptical model to fully heterogeneous marginal tails, with intermediate cluster structures that preserve within-group tail dependence.

5 The Scores and Fisher Information under Convolution- t Distributions

In this section, we derive the score ∇_t and the Fisher information matrix \mathcal{I}_t under each of the distributional specifications. The specifications differ primarily in how extreme observations are weighted when updating the correlation parameters, with the multivariate- t using a single global weight and the Cluster- t and Hetero- t using cluster- and asset-specific weights, respectively. The derivations below build on [Tong et al. \(2026\)](#), extending their framework to accommodate the block structure of the joint innovation vector.

To facilitate the derivations, we define the Jacobian matrix of the logarithmic transformation as $M_t = \partial \text{vec}(C_t) / \partial \gamma_t'$. Given the block-diagonal structure of the joint correlation matrix, $C_t = \text{blockdiag}(C_t^N, C_t^D)$, we introduce a $4n^2 \times 2n^2$ embedding matrix P_M that inserts rows of zeros corresponding to the cross-block zero entries. The full Jacobian is then constructed as $M_t = P_M \text{blockdiag}(M_t^N, M_t^D)$, where $M_t^N = \partial \text{vec}(C_t^N) / \partial \gamma_t^{N'}$ and $M_t^D = \partial \text{vec}(C_t^D) / \partial \gamma_t^{D'}$ are the Jacobians of the respective $n \times n$ sub-blocks. \otimes is the Kronecker product. We use the shorthand $A \oplus B = A \otimes B + B \otimes A$, as in [Creal, Koopman, and Lucas \(2011\)](#).

5.1 Case 1: The Multivariate- t Specification

If Z_t follows a $2n$ -dimensional (standardized) multivariate- t distribution with a single degree-of-freedom ν , the score with respect to γ_t takes the form:

$$\nabla_t^{MT} = \frac{1}{2} M_t' \left(C_t^{-1} \otimes C_t^{-1} \right) \left[W_t \text{vec} (Z_t Z_t') - \text{vec} (C_t) \right], \quad (9)$$

where $W_t = (\nu + 2n) / (\nu - 2 + Z_t' C_t^{-1} Z_t)$ acts as a global scaling factor that down-weights large Mahalanobis distances in the score. The Gaussian specification arises as the limiting case $\nu \rightarrow \infty$ under which $W_t \rightarrow 1$. Unlike the multivariate- t case, the Gaussian score assigns uniform weight to all observations regardless of the realized Mahalanobis distance, making it unbounded and sensitive to extreme shocks.

Due to the block-diagonal structure of C_t , the joint score under both specifications partitions into overnight and intraday components:

$$\nabla_t = \left(\nabla_t^{N'}, \nabla_t^{D'} \right)', \quad \text{where} \quad \nabla_t^c = \frac{1}{2} (M_t^c)' \left((C_t^c)^{-1} \otimes (C_t^c)^{-1} \right) \left[W_t \text{vec} (Z_t^c (Z_t^c)') - \text{vec} (C_t^c) \right], \quad (10)$$

for $c \in \{N, D\}$. Under the multivariate- t distribution, both ∇_t^N and ∇_t^D share the scaling weight W_t , which incorporates both Z_t^N and Z_t^D . An extreme overnight shock would decrease the total weight W_t . This cross-session coupling may lead to inefficient score updates when tail risks differ substantially across trading sessions.

The total Fisher information matrix decomposes as:

$$\mathcal{I}_t^{MT} = \begin{pmatrix} \mathcal{I}_N & \mathbf{0} \\ \mathbf{0} & \mathcal{I}_D \end{pmatrix} + \frac{\phi-1}{4} \mathcal{I}_{ND} \mathcal{I}_{ND}', \quad \text{where} \quad \mathcal{I}_c = \frac{\phi}{4} (M_t^c)' \left[\left((C_t^c)^{-1} \otimes (C_t^c)^{-1} \right) H_n \right] M_t^c, \quad (11)$$

for $c \in \{N, D\}$, with $\phi = \frac{\nu+2n}{\nu+2n+2}$ under the multivariate- t distribution and $\phi = 1$ under the Gaussian. $H_n = I_{n^2} + K_n$ and K_n is the commutation matrix. The cross-session term is given by $\mathcal{I}_{ND} = M_t' \text{vec} (C_t^{-1})$. Under the Gaussian specification, $\phi = 1$ and the coupling term $\frac{\phi-1}{4} \mathcal{I}_{ND} \mathcal{I}_{ND}'$ vanishes identically, so the Fisher information is exactly block-diagonal and the two sessions are fully decoupled.

5.2 Case 2: The Cluster- t Specification

The Cluster- t specification addresses the coupling problem in multivariate- t by allowing a predefined partition of assets into independent clusters, each carrying its own degrees-of-freedom parameter. In its simplest form, this specification groups variables by trading session, treating overnight and intraday innovations as two independent multivariate- t vectors. Under this session-level partition, the score for each session $c \in \{N, D\}$ follows the same functional form as the multivariate- t in Section 5.1, but is updated using a session-specific scaling weight W_t^c and degrees-of-freedom ν_c . This ensures that an extreme overnight shock no longer distorts the intraday parameter updates.

More generally, our framework allows for a more precise partition within each session. Suppose the n assets within session $c \in \{N, D\}$ are grouped into K sector-based clusters, with sector k containing n_k assets and $\sum_{k=1}^K n_k = n$. Define the orthogonalized shocks as $U_t^c = (C_t^c)^{-1/2} Z_t^c$ and partition them into K subvectors $U_{k,t}^c$. Each subvector follows an independent multivariate- t distribution with session- and sector-specific degrees-of-freedom parameter $\nu_{k,c}$.

Following Theorem 2 of [Tong et al. \(2026\)](#), the score for session c takes the form:

$$\nabla_t^{c,CT} = (M_t^c)' (\Omega_t^c)' \left[\sum_{k=1}^K W_{k,t}^c \text{vec} \left(E_k U_{k,t}^c (U_t^c)' \right) - \text{vec} (I_n) \right], \quad \text{where} \quad W_{k,t}^c = \frac{\nu_{k,c} + n_k}{\nu_{k,c} - 2 + (U_{k,t}^c)' U_{k,t}^c} \quad (12)$$

for $k = 1, \dots, K$, $E_k \in \mathbb{R}^{n \times n_k}$ is the embedding matrix that maps the k -th sector subvector into the full n -dimensional vector, so that E_k' selects the k -th sector from the full vector, and $\Omega_t^c = (I_n \otimes (C_t^c)^{-1/2}) ((C_t^c)^{1/2} \oplus I_n)^{-1}$.

This localized weighting scheme is the key feature of the Cluster- t specification. An extreme shock in sector k reduces the sector-specific $W_{k,t}^c$ and hence down-weights the score contribution associated with that sector, rather than globally down-weighting all sector contributions. Under the multivariate- t , by contrast, a single extreme shock depresses the global weight W_t and distorts the score updates for all assets simultaneously. When $K = 1$, the score collapses to the session-level case with a single weight $W_t^c = \frac{\nu_c + n}{\nu_c - 2 + (U_t^c)' U_t^c}$ for $c \in \{N, D\}$.

Since the overnight and intraday cluster systems are independent under the session-separated

convolution- t specification, the Fisher information is block-diagonal across sessions:

$$\mathcal{I}_t^{CT} = \begin{pmatrix} \mathcal{I}_N^{CT} & \mathbf{0} \\ \mathbf{0} & \mathcal{I}_D^{CT} \end{pmatrix}, \quad \text{where} \quad \mathcal{I}_c^{CT} = (M_t^c)' (\Omega_t^c)' (K_n + \Upsilon_K^c) \Omega_t^c M_t^c, \quad \Upsilon_K^c = \sum_{k=1}^K \Psi_k^c \quad (13)$$

for $c \in \{N, D\}$, where $\Psi_k^c = \psi_k^c (I_n \otimes J_k) + (\phi_k^c - \psi_k^c) (J_k \otimes J_k) + (\phi_k^c - 1) [(J_k \otimes J_k) K_n + \text{vec}(J_k) \text{vec}(J_k)']$, where $J_k = E_k E_k'$, $\phi_k^c = \frac{\nu_{k,c} + n_k}{\nu_{k,c} + n_k + 2}$, and $\psi_k^c = \phi_k^c \frac{\nu_{k,c}}{\nu_{k,c} - 2}$. This block-diagonal structure follows directly from the mutual independence of clusters across sessions imposed in Section 4.

5.3 Case 3: The Hetero- t Specification

The Hetero- t distribution is the limiting case in which each asset within each session forms its own independent cluster ($K = n$, $n_k = 1$ for all k). This gives every asset its own degrees-of-freedom parameter $\nu_{j,c}$, providing maximum flexibility in tail modeling.

The score takes the same form as in Section 5.2 with $K = n$. Since each cluster contains a single asset, the sector-level weight reduces to $W_{j,t}^c = (\nu_{j,c} + 1) / \{\nu_{j,c} - 2 + (U_{j,t}^c)^2\}$, $j = 1, \dots, n$. Here, $U_{j,t}^c$ is the j -th element of U_t^c . The score then becomes:

$$\nabla_t^{c,HT} = (M_t^c)' (\Omega_t^c)' \left[\sum_{j=1}^n W_{j,t}^c \text{vec} \left(E_j U_{j,t}^c (U_t^c)' \right) - \text{vec} (I_n) \right], \quad (14)$$

where E_j is the $n \times 1$ selection vector with unity in the j -th position and zeros elsewhere.

The Fisher information matrix retains the same block-diagonal structure as in the Cluster- t specification. The inner matrix Υ_n^c simply adapts to the asset-level partition as $\Upsilon_n^c = \sum_{j=1}^n \Psi_j^c$, where Ψ_j^c is computed using the formulas from Section 5.2 by setting $n_k = 1$ and replacing the sector index k with the asset index j .

5.4 The Key to High Dimensions: Canonical Representation of Block Structure

The analytical scores and information matrices derived above are formulated for the unrestricted $n \times n$ session-specific correlation matrices, C_t^N and C_t^D . However, when the number of assets n is large, updating the unrestricted parameter vectors $\gamma_t^N, \gamma_t^D \in \mathbb{R}^{n(n-1)/2}$ is still computationally difficult.

Although the block structure reduces the number of free parameters per session, computing the condensed score $\nabla_{\eta,t}^c$ still requires differentiating through the full $n \times n$ correlation matrix. We employ the canonical representation derived in Archakov and Hansen (2024), where any block correlation matrix can be decomposed as $C_t^c = QD_t^cQ'$. Here, Q is a time-invariant orthogonal matrix determined solely by the cluster sizes, and D_t^c is a block-diagonal matrix taking the form:

$$D_t^c = \text{blockdiag} \left(A_t^c, \lambda_{1,t}^c I_{n_1-1}, \dots, \lambda_{K,t}^c I_{n_K-1} \right). \quad (15)$$

Since the eigenvalues $\lambda_{k,t}^c$ are deterministic functions of the elements in A_t^c , the dynamic properties of the entire $n \times n$ correlation matrix C_t^c are entirely captured by the lower-dimensional $K \times K$ symmetric positive definite matrix A_t^c , for $c \in \{N, D\}$. The chain rule gives $\nabla_{\eta,t}^c = \Pi'_{A,c} \nabla_{A,t}^c$ for $c \in \{N, D\}$, where $\nabla_{A,t}^c = \partial \ell_t^c / \partial \text{vec}(A_t^c)$ is the score with respect to A_t^c . Closed-form expressions for both quantities under the multivariate- t , Cluster- t , and Hetero- t specifications are provided in Theorems 3-5 of Tong et al. (2026). The transition matrix $\Pi_{A,c} = \frac{\partial \text{vec}(A_t^c)}{\partial \eta_t^c}$ is given by:

$$\Pi_{A,c} = \left[\Gamma_{A,c} - \Gamma_{A,c} E_d' \left(\Phi_c^{-1} + E_d \Gamma_{A,c} E_d' \right)^{-1} E_d \Gamma_{A,c} \right] (\Lambda_n \otimes \Lambda_n) D_K, \quad (16)$$

where $\Gamma_{A,c} = \partial \text{vec}(A_t^c) / \partial \text{vec}(\log A_t^c)$, Φ_c is a $K \times K$ diagonal matrix with $\Phi_{c,kk} = \lambda_{k,t}^c (n_k - 1)$, and $\Lambda_n = \text{diag}(\sqrt{n_1}, \dots, \sqrt{n_K})$, E_d is an elimination matrix, and D_K is the duplication matrix. Evaluating $\Pi_{A,c}$ requires inverting only a $K \times K$ matrix, which keeps the model computationally tractable even in high dimensions.

Stacking the session-specific components gives $\nabla_{\eta,t} = (\nabla_{\eta,t}^{N'}, \nabla_{\eta,t}^{D'})'$, with $\nabla_{\eta,t}^c = \Pi'_{A,c} \nabla_{A,t}^c$ and $\mathcal{I}_{\eta,t}^c = \Pi'_{A,c} \mathcal{I}_{A,t}^c \Pi_{A,c}$, where $c \in \{N, D\}$. For the session-separated convolution- t specifications, $\mathcal{I}_{\eta,t}$ remains block-diagonal, so the overnight and intraday parameters can be updated separately. In the common multivariate- t case, the additional coupling term in the Fisher information remains.

6 Benchmark Model: DCC-GARCH Model

We use the Dynamic Conditional Correlation (DCC) GARCH model of Engle (2002), implemented through the corrected DCC (cDCC) specification of Aielli (2013), as a benchmark. We adapt the

cDCC specification to the joint overnight-intraday innovation vector $Z_t = (Z_t^{N'}, Z_t^{D'})'$ obtained from the first-stage Coupled EGARCH model. In the cDCC framework, the conditional correlation matrix is formulated as

$$C_t = \Lambda_{Q_t}^{-1/2} Q_t \Lambda_{Q_t}^{-1/2},$$

where Q_t is a $2n \times 2n$ symmetric positive definite matrix, and Λ_{Q_t} is the diagonal matrix containing the diagonal elements of Q_t . The dynamic properties of C_t are governed by the evolution of Q_t , which is updated via

$$Q_{t+1} = (\iota' - \alpha - \beta) \odot \bar{C} + \beta \odot Q_t + \alpha \odot \left(\Lambda_{Q_t}^{1/2} Z_t Z_t' \Lambda_{Q_t}^{1/2} \right), \quad (17)$$

where ι is a $2n \times 1$ vector of ones, \odot denotes the Hadamard product, and \bar{C} is the unconditional sample correlation matrix of Z_t . The parameter matrices α and β capture the innovation impact and persistence of the correlation dynamics, respectively. The diagonal elements of C_t are normalized to one by construction.

To make the benchmark comparable with the score-driven models, we evaluate the DCC model under the same main distributional specifications. Under the Gaussian benchmark, $Z_t | \mathcal{F}_t \sim N(0, C_t)$. Under the multivariate- t benchmark, $Z_t | \mathcal{F}_t \sim t_{2n, \nu}^{\text{std}}(0, C_t)$, so all overnight and intraday innovations share a common degrees-of-freedom parameter. Under the session-level Cluster- t benchmark, we write $Z_t = C_t^{1/2} U_t$, where $U_t = (U_t^{N'}, U_t^{D'})'$, $U_t^N \sim t_{n, \nu_N}^{\text{std}}(0, I_n)$, $U_t^D \sim t_{n, \nu_D}^{\text{std}}(0, I_n)$, and the two session components are mutually independent. This specification allows overnight and intraday innovations to have different tail thickness while retaining the DCC correlation update.

7 Six-Asset Empirical Application

This section presents a detailed empirical application using six U.S. equities from two industrial sectors. The small cross section allows us to examine the main mechanisms of the proposed model in detail: session-level tail heterogeneity, sector-level tail clustering, unrestricted versus block correlation dynamics, and out-of-sample predictive performance.

Table 1: Descriptive Statistics

Asset	Session	Mean (Ann., %)	Std. Dev. (Ann., %)	Skewness	Kurtosis
CVX	Total	5.2371	28.5322	-0.5027	24.4274
	Night	5.2930	15.9007	-1.0612	34.0504
	Day	-0.0559	22.3116	-0.3489	17.4820
APA	Total	-3.6940	50.1603	-3.1880	84.7365
	Night	15.2066	28.1480	-2.4121	92.1604
	Day	-18.9005	39.4028	-0.8950	17.1931
DVN	Total	-0.6411	45.3060	-0.8529	22.1656
	Night	13.7665	25.4334	-3.0507	77.1893
	Day	-14.4076	36.3537	-0.0588	7.3408
MSFT	Total	13.8102	27.1190	-0.0553	12.4788
	Night	6.3938	16.0672	-0.3731	28.4753
	Day	7.4164	21.1623	0.0025	7.5876
INTC	Total	-0.7026	33.0562	-1.0092	19.2634
	Night	-4.6812	20.2724	-3.6139	69.5382
	Day	3.9786	25.2623	0.1255	6.7911
CSCO	Total	5.6078	28.0333	-0.4621	15.2679
	Night	-1.7776	18.2802	-1.7500	43.2764
	Day	7.3854	21.1650	-0.1789	8.2608

Note: This table reports descriptive statistics. Mean and Std. Dev. are annualized percentages, obtained by multiplying the sample mean by 252×100 and the sample standard deviation by $\sqrt{252} \times 100$, respectively. Kurtosis denotes raw kurtosis. Total, Overnight, and Intraday refer to close-to-close, close-to-open, and open-to-close returns.

7.1 Data and Descriptive Statistics

We begin with six major U.S. stocks from two industrial sectors. The Energy sector is represented by Chevron (CVX), APA Corporation (APA), and Devon Energy (DVN), and the Information Technology sector by Microsoft (MSFT), Intel (INTC), and Cisco (CSCO). The two sectors differ in their information environments: energy stocks are more exposed to global commodity and macroeconomic news, while technology stocks are more sensitive to firm-specific announcements, including earnings and guidance releases that may occur outside regular trading hours. This contrast motivates the sector-based block structure imposed on the correlation matrix and the sector-based clustering in the convolution- t distribution. The sample spans from January 1, 2005, to December 31, 2024, with a total of $T = 5,032$ observations. Daily stock price data are from the Center for Research in Security Prices (CRSP) database, and all total, overnight, and intraday returns are computed as logarithmic returns.

Table 1 reports the descriptive statistics. Average returns are small at the daily frequency, but annualized means reveal clear session-level and sectoral differences. Energy stocks have higher average

Table 2: Session Correlations of Standardized Innovations

	Energy Sector			Technology Sector		
	CVX	APA	DVN	MSFT	INTC	CSCO
CVX	1.000	0.780	0.809	0.430	0.407	0.450
APA	0.604	1.000	0.834	0.378	0.352	0.379
DVN	0.656	0.729	1.000	0.407	0.370	0.403
MSFT	0.382	0.252	0.272	1.000	0.483	0.454
INTC	0.363	0.261	0.289	0.554	1.000	0.416
CSCO	0.409	0.295	0.324	0.582	0.555	1.000

Note: This table presents the sample correlation matrices of standardized innovations for six assets. The upper triangular part displays correlations of standardized overnight innovations; the lower triangular part displays correlations of standardized intraday innovations. Off-diagonal sector blocks correspond to cross-sector correlations.

overnight returns than intraday returns: APA shows an annualized overnight mean of 15.21% versus an intraday mean of -18.90%, and DVN shows 13.77% versus -14.41%. Technology stocks display more heterogeneous patterns, with MSFT earning positive average returns in both sessions and CSCO showing a negative overnight mean but a positive intraday mean.

Intraday returns have higher annualized standard deviations than overnight returns for all six assets. For example, CVX has an intraday standard deviation of 22.31% compared with 15.90% overnight, and MSFT has 21.16% intraday versus 16.07% overnight. This reflects the concentration of trading activity during market hours.

The most pronounced difference across sessions appears in tail behavior. Overnight kurtosis is extreme, reaching 92.16 for APA, 77.19 for DVN, and 69.54 for INTC, whereas intraday kurtosis is much lower, ranging from 6.79 (INTC) to 17.49 (CVX). This session-level difference in tail thickness is consistent with the tail heterogeneity that motivates the convolution- t framework. Overnight returns also tend to be more negatively skewed, but the main empirical feature for our model is the stronger heavy-tailed behavior of overnight returns.

Table 2 presents the static correlation matrices of the standardized innovations, with overnight innovation correlations in the upper triangle and intraday innovation correlations in the lower triangle.

Within-sector correlations are substantially higher than cross-sector correlations in both sessions. For the Energy sector, within-sector correlations range from 0.780 to 0.834 for overnight innovations and from 0.604 to 0.729 for intraday innovations. For the Information Technology sector, within-sector correlations range from 0.416 to 0.483 for overnight innovations and from 0.554 to 0.582 for intraday

Table 3: Mean Equation Estimates

Asset	Parameter Estimates						
	μ_N	μ_D	δ	ϕ_{11}	ϕ_{12}	ϕ_{21}	ϕ_{22}
Energy Sector							
CVX	0.0227 (0.0096)	-0.0058 (0.0154)	0.0636 (0.0227)	-0.0223 (0.0152)	0.0083 (0.0099)	0.0304 (0.0223)	-0.0354 (0.0152)
APA	0.0357 (0.0151)	-0.0755 (0.0260)	0.0162 (0.0309)	-0.0104 (0.0142)	0.0240 (0.0092)	0.0265 (0.0251)	-0.0029 (0.0155)
DVN	0.0572 (0.0140)	-0.0641 (0.0255)	0.0134 (0.0266)	-0.0098 (0.0148)	0.0231 (0.0090)	0.0165 (0.0251)	-0.0259 (0.0147)
Technology Sector							
MSFT	0.0228 (0.0127)	0.0413 (0.0150)	-0.0136 (0.0240)	0.0048 (0.0150)	-0.0461 (0.0132)	-0.0028 (0.0226)	-0.0309 (0.0145)
INTC	0.0017 (0.0150)	0.0093 (0.0182)	-0.0029 (0.0232)	0.0017 (0.0156)	-0.0311 (0.0148)	0.0631 (0.0189)	-0.0081 (0.0155)
CSCO	-0.0065 (0.0142)	0.0396 (0.0151)	-0.0363 (0.0221)	-0.0046 (0.0125)	-0.0284 (0.0143)	0.0721 (0.0174)	0.0040 (0.0165)

Note: This table reports the parameter estimates for the conditional mean equation. Parzen-kernel HAC standard errors, computed using the estimated conditional variances, are reported in parentheses.

innovations. Cross-sector correlations are lower in both sessions, ranging from 0.352 to 0.450 overnight and from 0.252 to 0.409 intraday.

The session-level pattern differs between sectors. For Energy, overnight innovation correlations exceed intraday innovation correlations across all within-sector pairs. For Technology, the pattern reverses: intraday innovation correlations exceed overnight innovation correlations. Cross-sector correlations are moderately higher overnight than intraday. These static estimates provide a preliminary characterization of the remaining dependence among standardized innovations. The model-based dynamic conditional correlations are discussed in Section 7.3.

7.2 Univariate Model Estimates

We estimate the Coupled EGARCH model asset by asset via QMLE. Table 3 reports the conditional mean estimates with Parzen-kernel HAC standard errors, while Table 4 reports the volatility-parameter estimates with robust QMLE standard errors. Three patterns are consistent across assets: high volatility persistence in both sessions, asymmetric leverage effects that vary across sessions and sectors, and cross-session spillovers with a visible sectoral pattern.

Table 3 reports the mean equation estimates. The parameters μ_N and μ_D are intercepts in the overnight and intraday mean equations, respectively. Energy stocks tend to exhibit positive overnight intercepts and negative intraday intercepts, whereas technology stocks show heterogeneous overnight intercepts and uniformly positive intraday intercepts. This suggests that return dynamics differ systematically across sectors, particularly in how returns are distributed across trading and non-trading hours.

The point estimates of the contemporaneous transmission parameter δ_i suggest a sectoral contrast. As implied by Equation 1, the intraday return $R_{i,t}^D$ depends on the term $\delta_i R_{i,t}^N$. Accordingly, positive estimates of δ_i indicate overnight–intraday continuation, whereas negative estimates indicate reversal. The estimates are positive for the energy stocks and negative for the technology stocks, although the statistical strength varies across assets. This suggests that overnight information in energy stocks tends to be reinforced during the trading day, while technology stocks exhibit partial correction of overnight price movements. Nevertheless, the magnitude of δ_i remains modest across both sectors.

The autoregressive coefficients in Φ_i are small across all assets. While significance varies, the economically small magnitudes suggest that lagged return dynamics play a limited role, whereas the contemporaneous transmission parameter δ_i captures the more visible within-day relation between overnight and intraday returns.

Table 4 presents the volatility equation estimates, divided into Panel A (Overnight Volatility) and Panel B (Intraday Volatility). Volatility persistence is high in both sessions. The autoregressive coefficients β^N and β^D are close to unity, indicating strong volatility clustering in both trading periods.

Leverage effects differ across sessions. Intraday volatility displays a standard leverage effect, with negative shocks generating larger increases in volatility. Overnight volatility shows more heterogeneity. Energy stocks retain the conventional leverage pattern, while some technology stocks show weaker or even reversed asymmetry during non-trading hours.

Cross-session spillovers are economically meaningful for many assets, especially through the magnitude spillover terms. The magnitude spillover parameters δ_2^N and δ_2^D are uniformly positive, indicating that large shocks in one session lead to increased volatility in the next. The signed spillover parameters δ_1^N and δ_1^D display more heterogeneous patterns. For energy stocks, δ_1^N is consistently negative across all three firms, suggesting that positive intraday shocks are associated with reduced

Table 4: Volatility Equation Estimates

	Energy Sector			Technology Sector		
	CVX	APA	DVN	MSFT	INTC	CSCO
Panel A: Overnight Volatility						
ω^N	-0.1890 (0.0330)	-0.1640 (0.0463)	-0.1803 (0.0314)	-0.0943 (0.0491)	-0.1528 (0.0803)	-0.1774 (0.0579)
β^N	0.9851 (0.0099)	0.9902 (0.0038)	0.9864 (0.0039)	0.9769 (0.0092)	0.9768 (0.0193)	0.9426 (0.0225)
τ_1^N	-0.0601 (0.0145)	-0.0664 (0.0212)	-0.0562 (0.0152)	-0.0473 (0.0190)	0.0577 (0.0297)	0.0056 (0.0573)
τ_2^N	0.1316 (0.0272)	0.1126 (0.0403)	0.1071 (0.0256)	0.0675 (0.0228)	0.0675 (0.0313)	0.0263 (0.0333)
δ_1^N	-0.0523 (0.0211)	-0.0357 (0.0189)	-0.0392 (0.0122)	0.0101 (0.0141)	-0.0324 (0.0308)	-0.0389 (0.0392)
δ_2^N	0.1080 (0.0206)	0.1162 (0.0319)	0.1375 (0.0273)	0.0653 (0.0550)	0.1544 (0.0915)	0.2207 (0.0775)
Panel B: Intraday Volatility						
ω^D	-0.1800 (0.0303)	-0.1213 (0.0303)	-0.1263 (0.0189)	-0.1555 (0.0249)	-0.1701 (0.0380)	-0.1619 (0.0286)
β^D	0.9799 (0.0119)	0.9894 (0.0036)	0.9858 (0.0038)	0.9692 (0.0107)	0.9736 (0.0109)	0.9662 (0.0094)
τ_1^D	-0.0503 (0.0289)	-0.0365 (0.0127)	-0.0304 (0.0077)	-0.0215 (0.0202)	-0.0223 (0.0162)	-0.0005 (0.0158)
τ_2^D	0.1506 (0.0169)	0.1109 (0.0289)	0.1198 (0.0201)	0.1308 (0.0273)	0.1767 (0.0432)	0.1856 (0.0264)
δ_1^D	-0.0555 (0.0175)	-0.0425 (0.0124)	-0.0335 (0.0086)	-0.0232 (0.0123)	0.0027 (0.0197)	-0.0476 (0.0263)
δ_2^D	0.0929 (0.0268)	0.0723 (0.0215)	0.0715 (0.0151)	0.1068 (0.0210)	0.0847 (0.0262)	0.0519 (0.0260)

Note: This table reports the volatility equation estimates. Panel A presents overnight volatility parameters; Panel B presents intraday volatility parameters. Robust standard errors are in parentheses.

overnight volatility. For technology stocks, δ_1^N is mixed in sign, offering little directional information. The pattern for δ_1^D is similarly heterogeneous across sectors, with most estimates negative but varying in magnitude and significance.

7.3 Multivariate Model Estimates

The multivariate model results are organized around two dimensions, the structure of which is illustrated in Figure 1. The first is the tail partition: a session-level specification where overnight and intraday innovations each share a single degrees-of-freedom parameter across all assets; a session-by-sector specification where Energy and Technology assets carry distinct tail parameters within each session; and an asset-level specification where each asset in each session has its own degrees-of-freedom parameter. The second dimension is whether a sector-based block structure is imposed on the correlation matrix. As an additional benchmark, we also consider a clustering based purely on sector classification, which

does not distinguish between overnight and intraday sessions. The results, reported in Appendix D, show that this specification performs worse than the session-based partitions, highlighting the importance of session-level heterogeneity in shaping tail behavior.

Tables 5 and 6 present results without the block structure, covering the full range of tail partitions within the score-driven framework alongside the DCC benchmark. Table 7 then imposes the block structure across all four tail specifications.

7.3.1 Baseline comparison

Table 5 compares the DCC model introduced in Section 6 with the score-driven framework under a common set of distributional assumptions. Both models are estimated with an unrestricted correlation matrix. For the heavy-tailed specifications, we consider both a common multivariate- t distribution and a session-level Cluster- t distribution, where tail thickness is allowed to differ between overnight and intraday innovations. We also report the Gaussian case as a limiting benchmark.

The score-driven framework consistently outperforms the DCC model under heavy-tailed specifications, while using fewer parameters. Under the Cluster- t , the total log-likelihood increases by 230 points, with 216 points coming from the overnight session and only 13 points from the intraday session. A similar pattern holds under the multivariate- t case. This asymmetry is consistent with the heavier tails of overnight returns, where extreme observations are more frequent and their treatment matters more for correlation updating.

Under the Gaussian specification, however, the ordering reverses for the overnight session: the score-driven model exhibits a deterioration of about 175 log-likelihood points, while the intraday component remains broadly comparable. When $W_t = 1$, the Gaussian score is unbounded, so extreme overnight shocks enter the correlation recursion without any down-weighting. This reversal under the Gaussian specification suggests that the score-driven advantage depends on an appropriate heavy-tailed specification, and further motivates the use of heavy-tailed distributions for overnight returns.

Comparing across distributions, moving from the Gaussian benchmark to the multivariate- t specification leads to large log-likelihood gains exceeding 6,000 points in both the DCC and score-driven models. These gains are entirely driven by the overnight component: the overnight log-likelihood

Table 5: Score-Driven and DCC Model Comparison

		Cluster- t (Session, $G = 2$)		Multivariate- t ($G = 1$)		Gaussian	
		Night	Day	Night	Day	Night	Day
Panel A: DCC Model							
μ	Q_{25}	0.1612	0.1275	0.2252	0.1054	0.0842	0.1202
	Q_{50}	0.2022	0.1719	0.2824	0.1352	0.1320	0.1682
	Max	0.7970	0.7945	0.9890	0.6846	0.5582	0.7562
β	Q_{25}	0.9861	0.9643	0.9690	0.9628	0.8595	0.9611
	Q_{50}	0.9875	0.9723	0.9792	0.9688	0.8779	0.9684
	Max	0.9928	0.9803	0.9942	0.9809	0.9284	0.9755
α	Q_{25}	0.0032	0.0113	0.0019	0.0122	0.0603	0.0138
	Q_{50}	0.0061	0.0141	0.0053	0.0137	0.0687	0.0171
	Max	0.0150	0.0258	0.0175	0.0226	0.1314	0.0247
ν		3.2336	10.791		5.6031		
p			116		115		114
ℓ			-65472		-67281		-73937
ℓ_N			-28955		-29512		-36935
ℓ_D			-36516		-37769		-37002
BIC			131932		135542		148846
Panel B: Score-driven Model							
μ	Q_{25}	0.1660	0.1284	0.2001	0.1092	0.0575	0.1265
	Q_{50}	0.1970	0.1736	0.2591	0.1474	0.1445	0.1681
	Max	0.8313	0.7923	0.8951	0.7462	0.6486	0.7817
β	Q_{25}	0.9910	0.9764	0.9403	0.9586	0.9002	0.9763
	Q_{50}	0.9950	0.9860	0.9946	0.9864	0.9892	0.9843
	Max	0.9995	0.9975	0.9995	0.9976	0.9986	0.9983
α	Q_{25}	0.0065	0.0073	0.0054	0.0065	0.0050	0.0058
	Q_{50}	0.0111	0.0107	0.0119	0.0114	0.0074	0.0110
	Max	0.0608	0.0330	0.0747	0.0218	0.0932	0.0376
ν		3.3305	10.958		5.6488		
p			92		91		90
ℓ			-65242		-67051		-74102
ℓ_N			-28739		-29284		-37110
ℓ_D			-36503		-37767		-36992
BIC			131268		134878		148971

Note: This table compares the DCC and score-driven models under the Cluster- t , multivariate- t , and Gaussian distributions, estimated without block structure. For DCC models, μ is the unconditional correlation parameter; for score-driven models, μ is the mean parameter in the transformed correlation space. The parameters β and α denote persistence and score sensitivity, respectively. Q_{25} and Q_{50} denote the 25th and 50th percentiles. ℓ_N and ℓ_D are the decomposed log-likelihoods for the overnight and intraday sessions. Gaussian specifications do not have a degrees-of-freedom parameter ν . The parameter count p includes only second-stage dependence and tail parameters used in the likelihood comparison and BIC calculation; first-stage Coupled EGARCH parameters are excluded. The larger p for the DCC specifications reflects the additional unconditional correlation parameters in the DCC recursion. Bold values indicate, within each panel (DCC or score-driven), the specification with the highest log-likelihood.

improves by more than 7,000 points, whereas the intraday component deteriorates under the common multivariate- t specification. This pattern reflects a limitation of imposing a single degrees-of-freedom parameter across sessions. Because overnight returns are substantially more heavy-tailed, the common tail parameter is largely driven by the overnight distribution. The resulting tail thickness is too heavy for intraday returns, leading to a poorer fit for that component. Thus, the common multivariate- t restriction forces a compromise that cannot fully capture the distinct tail behavior of the two sessions.

Allowing for tail heterogeneity across sessions directly addresses this limitation. Relative to the multivariate- t benchmark, the Cluster- t specification delivers sizable gains for both sessions. In the

score-driven model, the overnight log-likelihood improves by about 545 points, while the intraday component improves by about 1,264 points. A similar pattern is observed under DCC. The larger improvement for the intraday component reflects the correction of the excessively heavy tail imposed by the common multivariate- t specification. The estimated degrees of freedom reveal pronounced heterogeneity, with much heavier tails for overnight returns ($\nu_N = 3.3305$) than intraday returns ($\nu_D = 10.9582$), indicating that a single tail parameter is insufficient.

Finally, these gains are achieved without sacrificing parsimony. The score-driven Cluster- t model has fewer parameters than the DCC Cluster- t model and improves the BIC by about 664 points. Relative to the score-driven multivariate- t specification, it improves the BIC by about 3,610 points, confirming that the additional session-specific tail parameter is strongly supported by the information criterion.

7.3.2 Tail heterogeneity by session, sector, and asset

Table 6 presents three tail partition specifications within the score-driven framework. Score-Cluster- t (Session, $G = 2$) assigns a single degrees-of-freedom parameter to each session. Score-Cluster- t (Session \times Sector, $G = 4$) further partitions each session into Energy and Technology clusters. Score-Hetero- t (Session \times Asset, $G = 12$) allows for asset-level tail parameters. The correlation matrix remains unrestricted across all three cases.

Panel A reports dynamic parameters across specifications. The persistence β is uniformly high under all specifications, and the score sensitivity α shows similar stability. Panel B highlights a clear and persistent difference between overnight and intraday returns. Under the session-level specification, the overnight degrees of freedom are around 3.3, compared to roughly 11 for intraday returns. This gap remains when the partition is refined. At the sector level, overnight tails range from about 2.6 to 3.8, while intraday values cluster tightly around 9. The same separation appears in the Hetero- t specification: overnight degrees of freedom lie between 2.4 and 3.9, whereas intraday values fall between 6.6 and 8.3, with little overlap between the two. Regardless of how the partition is defined, overnight returns consistently exhibit much heavier tails. There is also some heterogeneity within the overnight session. Technology stocks display heavier tails than Energy stocks, with degrees of freedom around 2.6 versus 3.8 under the sector-level specification. This difference is consistent with the greater exposure of

Table 6: Score-Driven Models with Alternative Tail Partitions

	Score-Cluster- t (Session, $G = 2$)		Score-Cluster- t (Session \times Sector, $G = 4$)		Score-Hetero- t (Session \times Asset, $G = 12$)		
	Night	Day	Night	Day	Night	Day	
Panel A: Parameter Estimates							
μ	Q_{25}	0.1660	0.1284	0.1548	0.1270	0.1630	0.1302
	Q_{50}	0.1970	0.1736	0.1937	0.1728	0.2123	0.1780
	Max	0.8313	0.7923	0.9342	0.7967	0.8844	0.7897
β	Q_{25}	0.9910	0.9764	0.9754	0.9783	0.9849	0.9809
	Q_{50}	0.9950	0.9860	0.9909	0.9862	0.9921	0.9842
	Max	0.9995	0.9975	0.9997	0.9976	0.9993	0.9976
α	Q_{25}	0.0065	0.0073	0.0097	0.0077	0.0092	0.0074
	Q_{50}	0.0111	0.0107	0.0148	0.0114	0.0133	0.0104
	Max	0.0608	0.0330	0.0416	0.0325	0.1114	0.0320
Panel B: Degrees of Freedom							
ν_0	3.3305	10.958					
ν_1					3.8579	8.3447	
ν_2			3.7859	8.8750	3.1788	6.5741	
ν_3					3.4367	8.2856	
ν_4					2.6441	7.4232	
ν_5			2.6478	8.7139	2.5225	7.1219	
ν_6					2.3954	7.4850	
Panel C: Model Fit Diagnostics							
p	92		94		102		
ℓ	-65242		-64071		-64350		
ℓ_N	-28739		-27657		-27934		
ℓ_D	-36503		-36414		-36416		
BIC	131268		128943		129569		

Note: This table reports score-driven model estimates under three tail specifications without block structure. Score-Cluster- t (Session, $G = 2$) assigns one degrees-of-freedom parameter to each session; Score-Cluster- t (Session \times Sector, $G = 4$) partitions each session into Energy and Technology clusters; and Score-Hetero- t (Session \times Asset, $G = 12$) assigns each asset within each session its own degrees-of-freedom parameter. Q_{25} and Q_{50} denote the 25th and 50th percentiles. Under the session-level Cluster- t , ν_0 denotes the session-specific degrees of freedom. Under the session-by-sector Cluster- t , ν_1 – ν_3 share the Energy sector parameter and ν_4 – ν_6 share the Technology sector parameter. Under Hetero- t ($G = 12$), in each session column, ν_1, \dots, ν_6 correspond to CVX, APA, DVN, MSFT, INTC, and CSCO. ℓ_N and ℓ_D are decomposed log-likelihoods. The parameter count p includes only second-stage dependence and tail parameters used in the likelihood comparison and BIC calculation. Bold values indicate the superior specification.

technology firms to after-hours information releases. During the trading day, however, the two sectors look very similar, with degrees of freedom close to 9 in both cases.

In terms of model fit, the session-by-sector Cluster- t provides the best performance and lowest BIC. It improves the log-likelihood by 1,171 points relative to the session-level specification and by 279 points relative to the Hetero- t . The improvement over the session-level specification is mainly driven by the overnight component: moving from the session-level to the session-by-sector specification increases the overnight log-likelihood by about 1,082 points, while the intraday contribution is only 89 points. The weaker performance of the Hetero- t suggests that, in this six-asset application, the additional marginal tail flexibility does not compensate for the loss of a shared sector-level tail component. The session-by-sector Cluster- t provides a better balance between tail flexibility and dependence modeling.

Table 7: Block Correlation Structure Estimates

		Score-Block-Multivariate- t ($G = 1$)		Score-Block-Cluster- t Session ($G = 2$)		Score-Block-Cluster- t Session \times Sector ($G = 4$)		Score-Block-Hetero- t Session \times Asset ($G = 12$)	
		Night	Day	Night	Day	Night	Day	Night	Day
Panel A: Implied Correlations and Parameter Estimates									
ρ	ρ_{11}	0.7805	0.6244	0.7341	0.6667	0.7827	0.6697	0.7650	0.6670
	ρ_{12}	0.4539	0.2266	0.3821	0.2724	0.3543	0.2710	0.3475	0.2730
	ρ_{22}	0.6957	0.4464	0.6447	0.4948	0.5895	0.4971	0.5102	0.4957
μ	μ_{11}	0.7580	0.5724	0.6967	0.6209	0.7979	0.6258	0.7648	0.6218
	μ_{12}	0.2018	0.1097	0.1721	0.1294	0.1595	0.1285	0.1590	0.1285
	μ_{22}	0.6151	0.3822	0.5662	0.4210	0.5108	0.4253	0.4204	0.4238
β	β_{11}	0.9929	0.9893	0.9919	0.9842	0.9876	0.9816	0.9864	0.9829
	β_{12}	0.9735	0.9864	0.9814	0.9830	0.9789	0.9820	0.9811	0.9829
	β_{22}	0.9138	0.9782	0.9349	0.9827	0.9603	0.9800	0.9332	0.9809
α	α_{11}	0.0293	0.0255	0.0338	0.0318	0.0452	0.0340	0.0454	0.0336
	α_{12}	0.0891	0.0236	0.0624	0.0388	0.0792	0.0407	0.0685	0.0394
	α_{22}	0.0531	0.0322	0.0549	0.0348	0.0454	0.0393	0.0787	0.0387
Panel B: Degrees of Freedom									
ν_0		5.6532		3.3450	10.951				
ν_1								3.9607	9.0622
ν_2						3.8109	8.7091	3.1909	6.3936
ν_3								3.3801	7.9721
ν_4								2.6281	7.7632
ν_5						2.6515	8.8394	2.5188	7.2765
ν_6								2.4063	7.2252
Panel C: Model Fit Diagnostics									
p		19		20		22		30	
ℓ		-67128		-65337		-64139		-64438	
ℓ_N		-29251		-28727		-27627		-27909	
ℓ_D		-37877		-36610		-36512		-36529	
BIC		134417		130845		128465		129132	

Note: This table reports score-driven model estimates under four specifications with a sector-based block structure imposed on the correlation matrix. ρ_{11} , ρ_{22} , and ρ_{12} denote implied unconditional correlations for intra-Energy, intra-Technology, and cross-sector pairs, respectively. μ , β , and α denote the corresponding condensed parameters, persistence parameters, and score sensitivity parameters. ν_0 denotes the global or session-specific degrees of freedom for models without cross-sectional tail clusters ($G = 1, 2$). Under the sector-based Cluster- t model ($G = 4$), ν_1 – ν_3 share the Energy-sector parameter and ν_4 – ν_6 share the Technology-sector parameter. Under Hetero- t ($G = 12$), in each session column, ν_1, \dots, ν_6 correspond to CVX, APA, DVN, MSFT, INTC, and CSCO. ℓ_N and ℓ_D are decomposed log-likelihoods. The parameter count p includes only second-stage dependence and tail parameters used in the likelihood comparison and BIC calculation. Bold values indicate the superior specification.

7.3.3 Block correlation structure and dynamic correlations

Table 7 imposes a sector-based block structure across all four tail specifications for comparison with the unrestricted results in Tables 5 and 6.

The results are closely aligned with those obtained under the unrestricted specifications. The multivariate- t provides a relatively poor fit, with a log-likelihood of $-67,128$ and an implied degrees-of-freedom of about 5.7. Allowing for session-specific tails increases the log-likelihood by about 1,791 points with only one additional tail parameter, and improves the BIC by about 3,572 points.

The ranking of tail partitions is unchanged after imposing the block structure. The session-by-sector Cluster- t again provides the best fit, improving the log-likelihood by 1,198 points relative to the

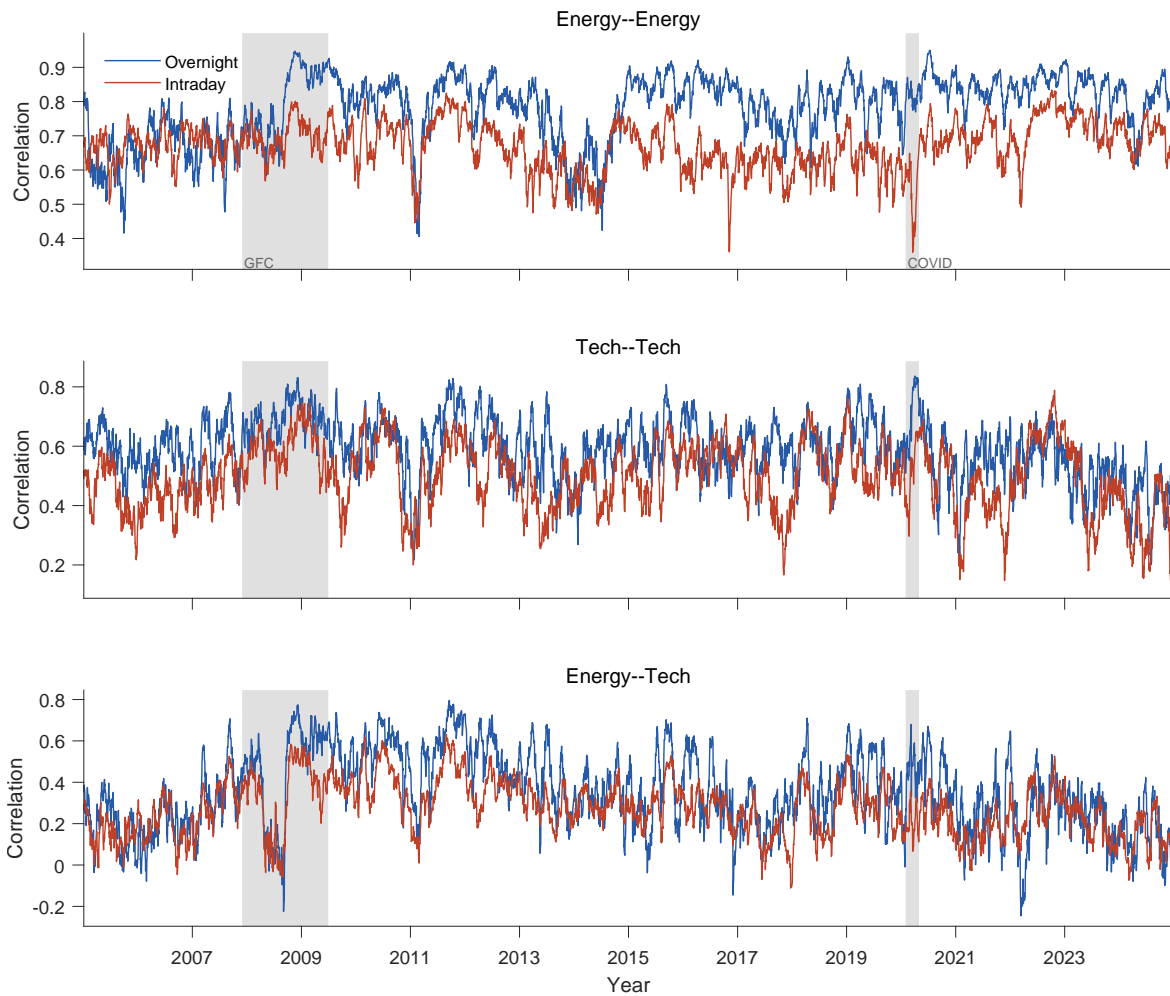


Figure 2: Dynamic Block Correlations: Score-Driven Model under Cluster- t Distribution
Note: This figure plots the estimated conditional block correlations from the Score-Block-Cluster- t model with session-by-sector tail clustering ($G = 4$). The upper, middle, and lower panels report Energy, Technology, and cross-sector correlations, respectively. Shaded areas indicate NBER-dated recessions.

session-level specification, with the gain concentrated in the overnight component. The fully flexible Hetero- t does not improve fit: its log-likelihood is 299 points lower than that of the session-by-sector Cluster- t , despite using more parameters.

Across all specifications, the block structure sharply reduces the number of parameters. Although the raw log-likelihood declines slightly, the loss is small relative to the large reduction in dimensionality, leading to improved BIC values. For the session-level Cluster- t , parameters fall from 92 to 20, and the BIC improves by 423 points. The session-by-sector specification yields an even larger BIC gain of 478, while the Hetero- t also benefits from a reduction in complexity, with a BIC improvement of 437 points.

Overall, these results reinforce a consistent message: imposing a simple sector-based block structure captures most of the relevant dependence in the data, substantially reducing model complexity while

preserving most of the fit, and often improving information-criterion performance.

To visualize the dependence dynamics implied by the preferred score-driven block specification, Figure 2 plots the estimated conditional block correlations for overnight and intraday returns. Within the Energy sector, shown in the upper panel, overnight correlations are consistently higher than their intraday counterparts throughout the sample period, with the gap remaining stable across different market regimes. Both series rise sharply during the Great Recession, reflecting increased co-movement among energy stocks during periods of broad market stress, and briefly spike at the onset of the COVID-19 shock before returning toward pre-pandemic levels.

Within the Information Technology sector, shown in the middle panel, overnight conditional correlations exceed intraday conditional correlations for most of the sample. The two series also display pronounced time variation, with correlation increases around major market stress episodes. This pattern is consistent with the importance of after-hours information arrivals for technology firms, including earnings announcements and guidance releases, which can generate substantial overnight dependence dynamics.

Cross-sector correlations, shown in the lower panel, exhibit no systematic gap between overnight and intraday series, with the two lines frequently crossing over the sample. During the Great Recession, correlations increase markedly and become more volatile in both sessions. Outside crisis periods, cross-sector correlations remain moderate and time-varying, suggesting that sectoral segmentation captures an important component of the dependence structure while still allowing for changing common exposure across sectors.

7.4 Out-of-Sample Evaluation

For the six-asset sample, we estimate models using data from 2005 to 2021 and evaluate out-of-sample performance over the period from 2022 to 2024 ($T_{oos} = 753$). Table 8 reports the out-of-sample log-likelihoods of total return ℓ , overnight return ℓ_N , and intraday return ℓ_D , along with p -values from the Model Confidence Set (MCS) test of Hansen, Lunde, and Nason (2011). Models with an MCS p -value above 0.05 belong to the superior set of models (SSM).

The out-of-sample results are broadly consistent with the in-sample findings. Score-driven specifica-

Table 8: Out-of-Sample Performance

Model	Log-Likelihood Components			Complexity	Stat. Test
	ℓ_N	ℓ_D	ℓ	p	MCS p -value
Panel A: Gaussian Distribution					
DCC	-5694	-5577	-11271	114	0.000
Score-Full	-5708	-5575	-11283	90	0.000
Panel B: Multivariate-t Distribution ($G = 1$)					
DCC	-4766	-5637	-10404	115	0.000
Score-Full	-4713	-5625	-10338	91	0.000
Score-Block	-4688	-5624	-10312	19	0.000
Panel C: Cluster-t Distribution (Session, $G = 2$)					
DCC	-4678	-5475	-10153	116	0.000
Score-Full	-4629	-5470	-10099	92	0.000
Score-Block	-4613	-5486	-10099	20	0.000
Panel D: Cluster-t Distribution (Session \times Sector, $G = 4$)					
Score-Full	-4485	-5440	-9925	94	1.000
Score-Block	-4478	-5458	-9936	22	0.498
Panel E: Hetero-t Distribution (Session \times Asset, $G = 12$)					
Score-Full	-4577	-5450	-10027	102	0.002
Score-Block	-4555	-5469	-10024	30	0.002

Note: This table reports out-of-sample log-likelihoods for the forecasting period 2022–2024 ($T_{\text{os}} = 753$). Models are grouped by distributional assumptions, from Gaussian to Hetero- t . ℓ_N and ℓ_D are decomposed overnight and intraday log-likelihoods, respectively, and p denotes the number of parameters. The Model Confidence Set (MCS) test evaluates predictive ability based on out-of-sample log-likelihoods. Bold MCS values indicate models in the superior set (MCS p -value > 0.05); the globally optimal total log-likelihood is also bolded.

tions tend to outperform the DCC benchmark under heavy-tailed distributions, and all DCC models are excluded from the SSM. Under the Gaussian specification, both DCC and score-driven models perform poorly. Moving from the multivariate- t to the session-level Cluster- t leads to noticeable improvements in log-likelihood, indicating that allowing for tail heterogeneity across return components remains important for predictive performance.

The session-by-sector Cluster- t specifications in Panel D achieve the strongest out-of-sample performance. Score-Full-Cluster- t attains the highest total log-likelihood of $-9,925$ and an MCS p -value of 1.000. Score-Block-Cluster- t also enters the SSM with a p -value of 0.498 and achieves a competitive log-likelihood of $-9,936$ with only 22 second-stage parameters, reflecting the parsimony gains from the sector-based block structure. These two specifications are the only models not excluded by the MCS test at the 5% level.

The Hetero- t specifications in Panel E perform worse out-of-sample than the session-by-sector Cluster- t , with both Score-Full and Score-Block specifications excluded from the SSM. This suggests that, with only three assets per sector-session block, the gain from additional marginal tail flexibility does not compensate for the loss of a shared sector-level tail component. The result is consistent with the

in-sample evidence in Section 7.3: preserving sector-level tail structure is more valuable than assigning a separate tail parameter to each asset.

The six-asset application provides a detailed setting in which to examine session-level and sector-level tail heterogeneity, unrestricted versus block correlation dynamics, and predictive performance. We next turn to a larger cross section to assess whether the proposed block representation remains tractable in high-dimensional settings.

8 High-Dimensional Empirical Application with 100 Assets

The preceding section used a small cross section to examine the mechanisms of the proposed model in detail. This section studies a 100-asset application to evaluate scalability. The purpose is not to replace the six-asset analysis, but to show that the same framework remains computationally tractable and empirically informative in a substantially larger cross section.

8.1 Sample Construction

The high-dimensional sample consists of 100 U.S. equities grouped into ten sectors over the period 2005–2023. The earlier endpoint relative to the six-asset sample reflects the need to maintain a balanced panel with complete open and close price records for all selected firms. The full list of assets and their sector classifications is provided in Appendix Table A.1. Since unrestricted correlation models are computationally impractical in this dimension, the analysis focuses on score-driven block specifications under alternative tail partitions. While the diagnostic evidence for the block-diagonal cross-session restriction $C_t^{ND} = 0$ is based on the six-asset sample, the same restriction is maintained in the 100-asset application as a parsimonious parametric assumption for scalable estimation.

8.2 In-Sample Block Correlation Estimates

Table 9 reports the implied block correlations, dynamic parameters, degrees of freedom, and in-sample fit measures for the 100-asset sample under the score-driven block specifications.

The results show that the block structure remains computationally tractable in the larger cross section.

Table 9: High-Dimensional Block Correlation Estimates for the 100-Asset Sample

		Score-Block-Multivariate- t ($G = 1$)		Score-Block-Cluster- t Session ($G = 2$)		Score-Block-Cluster- t Session \times Sector ($G = 20$)		Score-Block-Hetero- t Session \times Asset ($G = 200$)	
		Night	Day	Night	Day	Night	Day	Night	Day
Panel A: Implied Correlations and Parameter Estimates									
ρ	Q25	0.4459	0.2558	0.3593	0.3025	0.3908	0.3176	0.3617	0.3126
	Q50	0.4494	0.2581	0.3621	0.3052	0.3955	0.3204	0.3665	0.3158
	Max	0.4589	0.2649	0.3719	0.3122	0.4066	0.3282	0.3807	0.3243
μ	Q25	0.0385	0.0292	0.0364	0.0278	0.0371	0.0327	0.0350	0.0323
	Q50	0.0447	0.0364	0.0412	0.0390	0.0423	0.0399	0.0400	0.0399
	Max	0.0541	0.0522	0.0508	0.0534	0.0630	0.0574	0.0492	0.0549
β	Q25	0.7916	0.9573	0.4052	0.8940	0.8955	0.8107	0.9218	0.7902
	Q50	0.8807	0.9835	0.8513	0.9827	0.9705	0.9303	0.9746	0.9402
	Max	1.0000	0.9975	1.0000	0.9999	0.9999	0.9976	0.9991	0.9997
α	Q25	0.0050	0.0044	0.0016	0.0041	0.0085	0.0102	0.0088	0.0084
	Q50	0.0143	0.0072	0.0056	0.0088	0.0239	0.0222	0.0150	0.0219
	Max	0.0714	0.0259	0.0432	0.0494	0.0678	0.0723	0.0777	0.0831
Panel B: Degrees of Freedom									
ν_0		8.7419		4.4947	14.3034				
ν_1						3.3976	11.4409	2.4095 [†]	5.9396 [†]
ν_2						3.3357	9.8658	2.5848 [†]	6.5395 [†]
ν_3						2.9988	10.5407	3.1785 [†]	8.4010 [†]
ν_4						3.4748	10.0935	2.6145 [†]	5.1442 [†]
ν_5						3.4525	12.2934	2.4448 [†]	6.0608 [†]
ν_6						3.2292	10.3155	2.9676 [†]	7.3385 [†]
ν_7						2.7113	7.7214	2.5563 [†]	5.5523 [†]
ν_8						3.3386	11.3982	2.4315 [†]	4.9518 [†]
ν_9						3.1948	10.8006	2.6636 [†]	6.2696 [†]
ν_{10}						3.1097	9.3772	2.5279 [†]	6.3601 [†]
Panel C: Model Fit Diagnostics									
p		331		332		350		530	
ℓ		-1124328		-1100451		-1042293		-989034	
ℓ_N		-515857		-514676		-456925		-408421	
ℓ_D		-608470		-585775		-585368		-580613	
BIC		2251459		2203716		2087551		1982558	

Note: This table reports score-driven model estimates for 100 assets grouped into ten sectors under a sector-based block correlation structure. Panel A summarizes the distribution of implied sector-pair correlations and condensed dynamic parameters across the lower-triangular sector-pair entries. Q25, Q50, and Max denote the 25th percentile, median, and maximum, respectively. ρ , μ , β , and α denote implied unconditional correlations, condensed long-run correlations, persistence parameters, and score sensitivity parameters, respectively. In Panel B, ν_0 denotes the global or session-specific degrees of freedom for models with $G = 1$ or $G = 2$, while ν_1, \dots, ν_{10} denote sector-specific degrees of freedom under the Session \times Sector Cluster- t model ($G = 20$). For the Session \times Asset Hetero- t model ($G = 200$), the reported ν_1, \dots, ν_{10} [†] are sector-level averages of asset-specific degrees of freedom. ℓ_N and ℓ_D are decomposed log-likelihoods. The parameter count p includes only second-stage dependence and tail parameters used in the likelihood comparison and BIC calculation. Bold values indicate the superior specification.

Allowing for more flexible tail heterogeneity leads to sizeable improvements in both log-likelihood and BIC. In particular, the Hetero- t specification delivers the best in-sample fit, with the highest total log-likelihood and the lowest BIC. This suggests that asset-level tail heterogeneity becomes more important as the cross-sectional dimension increases.

The estimated degrees of freedom reveal a clear session contrast. The session-level Cluster- t estimates differ in absolute magnitude from those in the six-asset application. This difference is expected

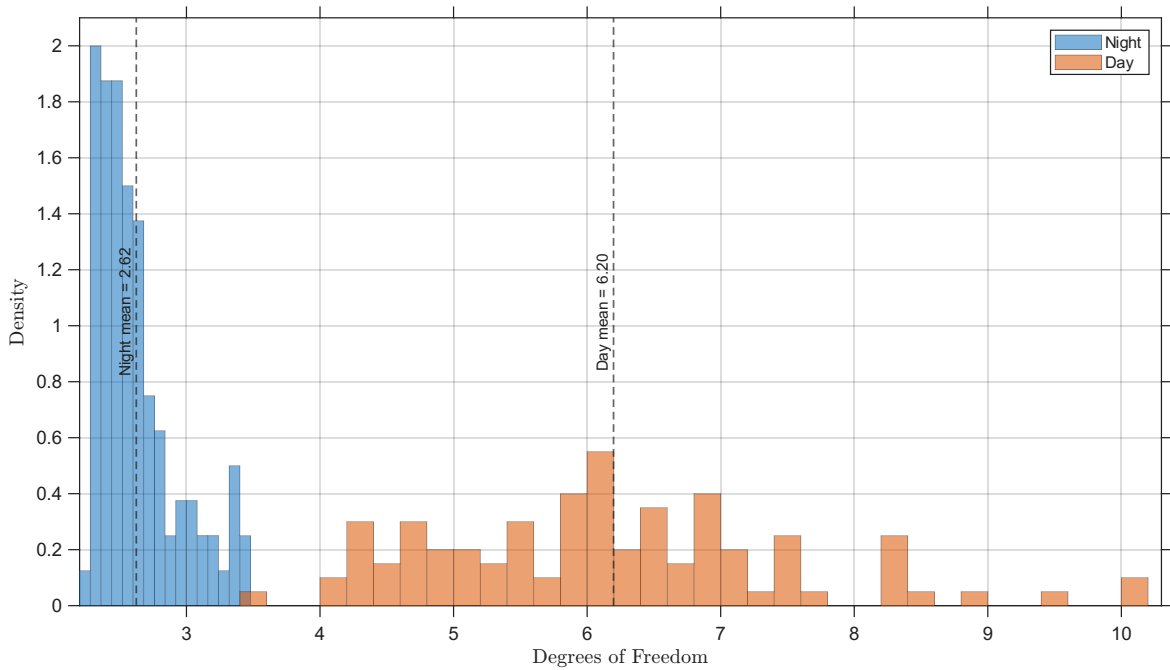


Figure 3: Distribution of Asset-Level Degrees of Freedom under the Hetero- t Specification
Note: This figure plots the distribution of asset-level degrees of freedom estimated under the Score-Block-Hetero- t specification in the 100-asset sample. Lower values correspond to heavier tails.

because the 100-asset sample covers a broader and more diversified set of firms and sectors. This session contrast remains visible under the more flexible specifications. Across the sector-level and asset-level specifications, the overnight degrees of freedom are systematically lower than their intraday counterparts, indicating heavier tails in overnight innovations. Figure 3 further illustrates this pattern under the Hetero- t specification. The overnight degrees of freedom are concentrated at lower values than the intraday degrees of freedom, providing visual evidence of stronger tail thickness in overnight innovations.

Overall, the 100-asset in-sample results confirm that the sector-based block structure provides a parsimonious and scalable representation of high-dimensional dependence. It substantially reduces the dimensionality of the correlation dynamics while preserving economically meaningful variation in both correlations and tail behavior.

8.3 Out-of-Sample Evaluation

We also examine out-of-sample performance in the 100-asset sample. Models are estimated using data from 2005–2020 and evaluated over 2021–2023. Since unrestricted correlation models are computationally impractical in this high-dimensional setting, the comparison focuses on score-driven

block models under alternative tail specifications. Table 10 reports both the likelihood-based evaluation and the correlation-based GMV portfolio evaluation.

For the portfolio evaluation, we construct correlation-based global minimum variance (GMV) portfolios using the model-implied forecasts of the joint split-session correlation matrix. Let $C_{m,t+1|t}$ denote the one-step-ahead conditional correlation matrix forecast from model m , where $C_{m,t+1|t} = \text{blockdiag}(C_{m,t+1|t}^N, C_{m,t+1|t}^D)$. Since the second-stage model is specified for standardized innovations, this exercise uses the forecast correlation matrix rather than the full return covariance matrix. The corresponding GMV weights are

$$\widehat{w}_{m,t+1|t} = \frac{C_{m,t+1|t}^{-1} \mathbf{1}}{\mathbf{1}' C_{m,t+1|t}^{-1} \mathbf{1}}.$$

The realized portfolio return is computed as $\widehat{w}'_{m,t+1|t} Z_{t+1}$, where $Z_{t+1} = (Z_{t+1}^N, Z_{t+1}^D)'$ denotes the vector of standardized overnight and intraday innovations. We compare models using the realized variance of these portfolio returns and apply the MCS test to the corresponding squared portfolio returns. This exercise is therefore interpreted as a correlation-based evaluation of dependence forecasts rather than a full volatility-scaled asset-allocation exercise.

The high-dimensional out-of-sample results broadly support the in-sample evidence. More flexible tail specifications improve predictive performance relative to the common multivariate- t benchmark, and the Hetero- t model delivers the highest total log-likelihood. It is also the only model retained in the superior set by the likelihood-based MCS test. The GMV results are consistent with this ranking: the Hetero- t model delivers the lowest realized variance and is retained in the superior set by the GMV MCS test. This out-of-sample evidence suggests that the additional flexibility of the Hetero- t specification captures persistent asset-level tail heterogeneity rather than merely fitting in-sample noise. In contrast to the six-asset benchmark, where the session-by-sector Cluster- t performs best, the 100-asset results suggest that asset-level tail heterogeneity becomes more valuable as the cross-sectional dimension increases.

Table 10: High-Dimensional Out-of-Sample Performance and GMV Evaluation

Model	Out-of-Sample Log-Likelihood Evaluation				GMV Performance		
	ℓ_N	ℓ_D	ℓ	p	MCS- p	RV	MCS- p
Panel A: Score-Block-Multivariate-t Distribution ($G = 1$)							
Score-Block	-86629	-98042	-184671	331	0.000	0.1519	0.013
Panel B: Score-Block-Cluster-t Distribution (Session, $G = 2$)							
Score-Block	-85938	-94512	-180450	332	0.000	0.1429	0.183
Panel C: Score-Block-Cluster-t Distribution (Session \times Sector, $G = 20$)							
Score-Block	-78624	-94627	-173250	350	0.000	0.1402	0.183
Panel D: Score-Block-Hetero-t Distribution (Session \times Asset, $G = 200$)							
Score-Block	-72665	-93679	-166344	530	1.000	0.1376	1.000

Note: This table reports out-of-sample log-likelihoods and GMV portfolio performance for the forecasting period 2021–2023. The models are estimated under a sector-based block correlation structure for 100 assets grouped into ten sectors. ℓ_N and ℓ_D denote the overnight and intraday log-likelihood components, respectively, and ℓ denotes the total out-of-sample log-likelihood. For the Score-Block-Multivariate- t model, ℓ is computed from the joint likelihood and therefore does not necessarily equal the sum of the reported decomposed components. The number of parameters is denoted by p . The log-likelihood MCS test is based on out-of-sample log-likelihood losses. The GMV realized variance is computed from the model-implied joint split-session correlation matrix, $C_t = \text{blockdiag}(C_t^N, C_t^D)$, and the standardized innovation vector $Z_t = (Z_t^N, Z_t^D)'$. The GMV MCS test is based on squared portfolio returns. Bold values indicate the highest log-likelihood, the lowest GMV realized variance, and models included in the superior set according to the corresponding MCS test.

9 Conclusion

This paper develops Split-Session Cluster GARCH, a model for heavy-tailed multivariate dependence in asset returns decomposed into overnight and intraday components. The model combines asset-specific Coupled EGARCH dynamics with a score-driven correlation model for standardized innovations. Tail heterogeneity is introduced through convolution- t distributions, allowing degrees of freedom to vary across clusters defined by trading sessions and economically meaningful asset groups. The correlation dynamics use the unconstrained correlation parameterization and the canonical block-correlation representation, preserving positive definiteness while improving scalability.

The empirical results show that separating overnight and intraday returns is important for modeling heavy-tailed dependence. In the six-asset application, overnight innovations are substantially more heavy-tailed than intraday innovations, with estimated degrees of freedom differing by roughly a factor of three. A common multivariate- t specification masks this session-level tail heterogeneity. Allowing separate tail parameters by session improves fit, and further partitioning tails by sector delivers additional gains concentrated mainly in the overnight component. These findings indicate that tail behavior varies along both time and cross-sectional dimensions.

The results also show that score-driven updating is most effective when paired with an appropriate heavy-tailed specification. Relative to traditional DCC models, score-driven specifications perform better under heavy-tailed distributions, especially for overnight returns, where extremes are more frequent. The clustered convolution- t specification localizes the impact of extremes through session- and group-specific tail weights.

The 100-asset application confirms that the framework remains feasible in a larger cross section. The block representation reduces the dependence system from the asset-pair level to the block-pair level while still allowing rich tail heterogeneity. In this setting, the block Hetero- t specification delivers the strongest in-sample and out-of-sample likelihood performance among the block models and also achieves the lowest realized variance in the GMV portfolio evaluation.

Overall, imposing a common tail structure can distort dynamic correlation modeling when tail behavior differs across sessions and asset groups. Split-Session Cluster GARCH addresses this issue by combining session-specific volatility dynamics, clustered heavy-tailed innovations, and scalable block-structured correlation dynamics. Future research could consider data-driven clustering, time-varying cluster memberships, broader asset universes, and high-dimensional asymptotic theory.

Appendix

A Composition of the 100-Asset Sample

Table A.1 lists the 100 stocks used in the high-dimensional analysis. The stocks are grouped by sector according to their sector classifications in the sample.

Table A.1

List of Stocks in the 100-Asset Sample

Sector	Stocks	Sector	Stocks
Information Technology	AAPL, ACN, ADBE, CRM, CSCO , IBM, INTC , MSFT , NVDA, ORCL, QCOM, TXN, XRX	Energy	APA , BKR, COP, CVX , DVN , HAL, MRO, NOV, OXY, SLB, WMB, XOM
Healthcare	ABT, AMGN, BAX, BMY, DHR, GILD, JNJ, LLY, MDT, MRK, PFE, TMO, UNH	Materials	APD, ECL, FCX, IP, SHW
Utilities	AEE, AEP, D, DUK, ETR, EXC, SO	Industrials	BA, CAT, EMR, FDX, GD, GE, HON, LMT, MMM, NSC, UNP, UPS
Financials	ALL, AXP, BAC, BK, C, COF, GS, JPM, MET, RF, USB, WFC	Consumer Staples	CL, COST, CPB, KO, MDLZ, MO, PEP, PG, WBA, WMT
Consumer Discretionary	AMZN, EBAY, F, HD, LOW, MCD, NKE, SBUX, TGT	Telecom. Services	CMCSA, DIS, DISH, NFLX, OMC, T, VZ

Note: This table reports the composition of the 100-asset sample by sector. Stocks are grouped according to their Global Industry Classification Standard (GICS) sector classifications. Bold entries indicate the six stocks used in the small sample.

B Diagnostic Test

Table B.1 reports diagnostic checks of residual contemporaneous cross-session dependence between the standardized overnight and intraday innovations. Since the Coupled EGARCH framework explicitly captures the most direct same-asset cross-session dependence through the transmission parameter δ_i and the coupled variance dynamics, the standardized residuals are expected to exhibit little remaining linear contemporaneous dependence across sessions.

Table B.1

Contemporaneous Correlation

Panel A: Same-Asset Cross-Session Correlations			
Asset	ρ_{ND}	t -stat (Parzen)	p -value
<i>Energy Sector</i>			
CVX	0.0060	0.411	0.681
APA	0.0218	1.118	0.263
DVN	0.0188	1.208	0.227
<i>Technology Sector</i>			
MSFT	0.0067	0.419	0.675
INTC	0.0299	1.789	0.074
CSCO	0.0140	0.811	0.417
Panel B: Cross-Asset Cross-Session Correlation Ranges			
Night sector / Day sector	Correlation range	t -stat range (Parzen)	p -value range
Energy / Energy	[0.0140,0.0656]	[0.989,4.195]	[0.000,0.323]
Energy / Technology	[-0.0083,0.0238]	[-0.564,1.391]	[0.164,0.986]
Technology / Energy	[0.0075,0.0380]	[0.517,2.561]	[0.010,0.605]
Technology / Technology	[-0.0047,0.0619]	[-0.252,4.089]	[0.000,0.801]

Note: Panel A reports same-asset Pearson correlations, $\rho(Z_{i,t}^N, Z_{i,t}^D)$. Panel B summarizes cross-asset cross-session correlations, $\rho(Z_{i,t}^N, Z_{j,t}^D)$ for $i \neq j$, grouped by the overnight and intraday asset sectors. Same-asset pairs are excluded from Panel B. HAC standard errors with the Parzen kernel and bandwidth $M = 5$ are used to compute the associated t -statistics and p -values. Values reported as 0.000 are smaller than 0.0005.

Consistent with this expectation, Panel A shows that the same-asset overnight-intraday correlations are uniformly small, with absolute values below 0.03. Using HAC standard errors with the Parzen kernel and bandwidth $M = 5$, none of these correlations is statistically significant at the 5% level. The largest same-asset estimate is observed for INTC, with a correlation of 0.0299, which is economically negligible.

Panel B further summarizes cross-asset cross-session correlations of the form $\rho(Z_{i,t}^N, Z_{j,t}^D)$ for $i \neq j$, grouped by the sector of the overnight asset and the sector of the intraday asset. These correlations

also remain small in magnitude. The within-sector cross-session ranges are [0.0140,0.0656] for Energy and [-0.0047,0.0619] for Technology, while the cross-sector ranges are [-0.0083,0.0238] for Energy overnight-Technology intraday pairs and [0.0075,0.0380] for Technology overnight-Energy intraday pairs. Based on Parzen-kernel HAC inference, across all 30 cross-asset cross-session pairs, 21 are statistically insignificant at the 5% level, and 27 have absolute correlations below 0.05. Even the largest cross-asset cross-session correlation, 0.0656, is much smaller than the within-session correlations in Table 2.

Overall, the evidence suggests that the remaining linear contemporaneous dependence between overnight and intraday standardized residuals is economically limited, which is consistent with the block-diagonal correlation specification adopted in the correlation model. These diagnostics are based on linear correlations and therefore should be interpreted as evidence on residual linear cross-session dependence; they do not test for nonlinear cross-session dependence or tail co-movement.

C The Score and Fisher Information for the General Specification

In this appendix, we provide the log-likelihood, the score vector, and the Fisher information matrix for the general $2n \times 2n$ joint conditional correlation matrix C_t under the multivariate- t and convolution- t distributions.

Following Archakov and Hansen (2021), we parameterize C_t using $\gamma_t = \text{vecl}(\log C_t)$, where $\text{vecl}(\cdot)$ stacks the strictly lower triangular elements of a matrix into a column vector. We define the Jacobian matrix as $M_t = \partial \text{vec}(C_t) / \partial \gamma_t'$. For brevity in the derivation, we omit the time subscript t in the following expressions.

C.1 The General Multivariate- t Distribution

Assume the $2n \times 1$ joint innovation vector Z follows a standardized multivariate- t distribution with ν degrees-of-freedom, $Z \sim t_\nu^{\text{std}}(\mathbf{0}, C)$. The conditional log-likelihood function is:

$$\ell(Z) = c_{\nu, 2n} - \frac{1}{2} \log |C| - \frac{\nu + 2n}{2} \log \left(1 + \frac{1}{\nu - 2} Z' C^{-1} Z \right), \quad (\text{C.1})$$

where $c_{\nu,2n}$ is the normalizing constant. Define $W = \frac{\nu+2n}{\nu-2+Z'C^{-1}Z}$. The score vector with respect to γ is

$$\nabla = \frac{\partial \ell}{\partial \gamma} = \frac{1}{2} M' \left(C^{-1} \otimes C^{-1} \right) [W \text{vec}(ZZ') - \text{vec}(C)]. \quad (\text{C.2})$$

The corresponding conditional Fisher information matrix $\mathcal{I} = \mathbb{E}[\nabla \nabla']$ is

$$\mathcal{I} = \frac{1}{4} M' \left[\phi \left(C^{-1} \otimes C^{-1} \right) H_{2n} + (\phi - 1) \text{vec}(C^{-1}) \text{vec}(C^{-1})' \right] M, \quad (\text{C.3})$$

where $\phi = \frac{\nu+2n}{\nu+2n+2}$, and $H_{2n} = I_{4n^2} + K_{2n}$, where K_{2n} is the $4n^2 \times 4n^2$ commutation matrix.

C.2 The General Convolution- t Distribution

We consider the more flexible Convolution- t distribution, which accommodates heterogeneous tail behaviors. The joint innovation vector is represented as $Z = C^{1/2}U$, where U consists of G independent multivariate t -distributed components U_g with dimension m_g and degrees-of-freedom ν_g . The log-likelihood function is

$$\ell(Z) = -\frac{1}{2} \log |C| + \sum_{g=1}^G \left[c_g - \frac{\nu_g + m_g}{2} \log \left(1 + \frac{U_g' U_g}{\nu_g - 2} \right) \right],$$

where $U_g = E_g' C^{-1/2} Z$ and $E_g \in \mathbb{R}^{2n \times m_g}$ is defined by $I_{2n} = (E_1, \dots, E_G)$. Define $W_g = (\nu_g + m_g) / (\nu_g - 2 + U_g' U_g)$. The score is

$$\nabla = M' \Omega' \nabla_s, \quad \nabla_s = \sum_{g=1}^G W_g \text{vec}(E_g U_g U_g') - \text{vec}(I_{2n}),$$

with $\Omega = (I_{2n} \otimes C^{-1/2})(C^{1/2} \oplus I_{2n})^{-1}$. The Fisher information matrix is $\mathcal{I} = M' \Omega' (K_{2n} + \Upsilon_G) \Omega M$, where $\Upsilon_G = \sum_{g=1}^G \Psi_g$ and

$$\Psi_g = \psi_g (I_{2n} \otimes J_g) + (\phi_g - \psi_g) (J_g \otimes J_g) + (\phi_g - 1) [(J_g \otimes J_g) K_{2n} + \text{vec}(J_g) \text{vec}(J_g)'] .$$

Here $J_g = E_g E_g'$, $\phi_g = (\nu_g + m_g) / (\nu_g + m_g + 2)$, and $\psi_g = \phi_g \nu_g / (\nu_g - 2)$.

D Sector-Based Clustering

As an alternative specification, we examine whether sector classification provides a better clustering structure than the session-based decomposition used in the main analysis. This comparison helps distinguish whether cross-sectional heterogeneity across industries or temporal heterogeneity across trading sessions is more important for tail behavior.

We estimate a sector-based Cluster- t model in which the orthogonalized innovation vector $U_t = C_t^{-1/2}Z_t \in \mathbb{R}^{2n}$ is partitioned by sectors rather than by sessions. Each sector forms an independent cluster containing both overnight and intraday innovations. For our sample of $n = 6$ assets, the partition is

$$U_{1,t} = \left[U_t^{N,\text{Energy}}, U_t^{D,\text{Energy}} \right]' \sim t_{\nu_1}^{\text{std}}(0, I_6), \quad U_{2,t} = \left[U_t^{N,\text{Tech}}, U_t^{D,\text{Tech}} \right]' \sim t_{\nu_2}^{\text{std}}(0, I_6),$$

where $U_t^{N,s}$ and $U_t^{D,s}$ denote overnight and intraday innovations for sector s from the partition of the orthogonalized innovation vector U_t , and ν_1, ν_2 are sector-specific degrees of freedom. Thus, shocks within a sector jointly determine the score downweighting, regardless of whether they occur overnight or intraday.

Table D.1 compares this sector-based partition with the baseline session-based specification. The results clearly favor the temporal decomposition: the sector-based model delivers a lower log-likelihood and a higher BIC. By pooling overnight and intraday innovations within each sector, it estimates intermediate degrees of freedom ($\nu_1 = 5.7955$ and $\nu_2 = 4.2819$), averaging severe overnight tails with milder intraday tails. This deterioration indicates that session-level heterogeneity is the primary dimension of tail variation. Sectoral heterogeneity remains important, but it is most informative when modeled within each trading session rather than by pooling overnight and intraday innovations within sectors.

Declaration of competing interest

The authors declare that they have no known competing financial interests or personal relationships that could have appeared to influence the work reported in this paper.

Table D.1: Session and Sector Comparison

		Score-Cluster- t (Session, $G = 2$)		Score-Cluster- t (Sector, $K = 2$)	
		Night	Day	Sector 1	Sector 2
Panel A: Parameter Estimates					
μ	Q_{25}	0.1660	0.1284	0.0201	0.0140
	Q_{50}	0.1970	0.1736	0.1012	0.0319
	Max	0.8313	0.7923	0.9999	0.7342
β	Q_{25}	0.9910	0.9764	0.9897	0.9134
	Q_{50}	0.9950	0.9860	0.9939	0.9713
	Max	0.9995	0.9975	1.0000	0.9969
α	Q_{25}	0.0065	0.0073	0.0018	0.0000
	Q_{50}	0.0111	0.0107	0.0043	0.0030
	Max	0.0608	0.0330	0.0299	0.0657
Panel B: Degrees of Freedom					
ν		3.3305	10.9582	5.7955	4.2819
Panel C: Model Fit Diagnostics					
p		92		92	
ℓ		-65242		-67057	
ℓ_N / ℓ_1		-28739		-32298	
ℓ_D / ℓ_2		-36503		-34758	
BIC		131268		134898	

Note: This table compares the session-based Cluster- t ($G = 2$) and sector-based Cluster- t ($K = 2$) specifications within the score-driven framework. μ denotes the mean parameter in the transformed correlation space, while β and α denote persistence and score sensitivity parameters, respectively. Q_{25} and Q_{50} denote the 25th and 50th percentiles. ℓ_N / ℓ_1 and ℓ_D / ℓ_2 are decomposed log-likelihoods under the corresponding session- or sector-level partitions. The parameter count p includes only second-stage dependence and tail parameters used in the likelihood comparison and BIC calculation. Bold values indicate the superior specification.

Data availability

The data are available from CRSP. Empirical code is available from the authors upon reasonable request.

Declaration of generative AI and AI-assisted technologies

During the preparation of this work the authors used OpenAI's ChatGPT in order to assist with language editing, LaTeX drafting, notation checks, and final-readiness review. After using these tools, the authors reviewed and edited the content as necessary and take full responsibility for the content of the publication.

References

Gian Piero Aielli. Dynamic conditional correlation: On properties and estimation. *Journal of Business & Economic Statistics*, 31(3):282–299, 2013. doi: 10.1080/07350015.2013.771027.

- Ilya Archakov and Peter Reinhard Hansen. A new parametrization of correlation matrices. *Econometrica*, 89(4):1699–1715, 2021. doi: 10.3982/ECTA16910.
- Ilya Archakov and Peter Reinhard Hansen. A canonical representation of block matrices with applications to covariance and correlation matrices. *Review of Economics and Statistics*, 106(4):1099–1113, July 2024. doi: 10.1162/rest_a_01258.
- Ilya Archakov, Peter Reinhard Hansen, and Asger Lunde. A multivariate realized GARCH model. *Journal of Econometrics*, 254:106040, March 2026. doi: 10.1016/j.jeconom.2025.106040.
- Michael J. Barclay and Terrence Hendershott. Price discovery and trading after hours. *The Review of Financial Studies*, 16(4):1041–1073, October 2003. doi: 10.1093/rfs/hhg030.
- Pierre Blanc, Rémy Chicheportiche, and Jean-Philippe Bouchaud. The fine structure of volatility feedback II: Overnight and intra-day effects. *Physica A: Statistical Mechanics and its Applications*, 402:58–75, May 2014. doi: 10.1016/j.physa.2014.01.047.
- Tim Bollerslev. Modelling the coherence in short-run nominal exchange rates: A multivariate generalized ARCH model. *The Review of Economics and Statistics*, 72(3):498–505, 1990. doi: 10.2307/2109358.
- Drew Creal, Siem Jan Koopman, and André Lucas. A Dynamic Multivariate Heavy-Tailed Model for Time-Varying Volatilities and Correlations. *Journal of Business & Economic Statistics*, 29(4): 552–563, October 2011. doi: 10.1198/jbes.2011.10070.
- Drew Creal, Siem Jan Koopman, and André Lucas. Generalized autoregressive score models with applications. *Journal of Applied Econometrics*, 28(5):777–795, August 2013. doi: 10.1002/jae.1279.
- Drew D. Creal and Ruey S. Tsay. High dimensional dynamic stochastic copula models. *Journal of Econometrics*, 189(2):335–345, December 2015. doi: 10.1016/j.jeconom.2015.03.027.
- Gianluca De Nard, Robert F. Engle, Olivier Ledoit, and Michael Wolf. Large dynamic covariance matrices: Enhancements based on intraday data. *Journal of Banking & Finance*, 138:106426, May 2022. doi: 10.1016/j.jbankfin.2022.106426.

- Geert Dhaene and Jianbin Wu. Incorporating overnight and intraday returns into multivariate GARCH volatility models. *Journal of Econometrics*, 217(2):471–495, August 2020. doi: 10.1016/j.jeconom.2019.12.013.
- Robert Engle. Dynamic conditional correlation: A simple class of multivariate generalized autoregressive conditional heteroskedasticity models. *Journal of Business & Economic Statistics*, 20(3):339–350, 2002. doi: 10.1198/073500102288618487.
- Robert Engle and Bryan Kelly. Dynamic equicorrelation. *Journal of Business & Economic Statistics*, 30(2):212–228, April 2012. doi: 10.1080/07350015.2011.652048.
- Robert F. Engle, Olivier Ledoit, and Michael Wolf. Large dynamic covariance matrices. *Journal of Business & Economic Statistics*, 37(2):363–375, April 2019. doi: 10.1080/07350015.2017.1345683.
- Kenneth R. French and Richard Roll. Stock return variances: The arrival of information and the reaction of traders. *Journal of Financial Economics*, 17(1):5–26, September 1986. doi: 10.1016/0304-405X(86)90004-8.
- Giulio Girardi and A. Tolga Ergün. Systemic risk measurement: Multivariate GARCH estimation of CoVaR. *Journal of Banking & Finance*, 37(8):3169–3180, 2013. doi: 10.1016/j.jbankfin.2013.02.027.
- Peter R. Hansen, Asger Lunde, and James M. Nason. The model confidence set. *Econometrica*, 79(2):453–497, 2011. doi: 10.3982/ECTA5771.
- Peter Reinhard Hansen and Chen Tong. Convolution- t distributions. *Journal of Econometrics*, 254:106212, March 2026. doi: 10.1016/j.jeconom.2026.106212.
- Igor Honig and Felix Kircher. Large dynamic covariance matrices and portfolio selection with a heterogeneous autoregressive model. *Journal of Banking & Finance*, 178:107505, 2025. doi: 10.1016/j.jbankfin.2025.107505.
- Long Kang and Simon H. Babbs. Modeling overnight and daytime returns using a multivariate generalized autoregressive conditional heteroskedasticity copula model. *The Journal of Risk*, 14(4):35–63, 2012. doi: 10.21314/JOR.2012.246.

- Donggyu Kim, Minseok Shin, and Yazhen Wang. Overnight GARCH-Itô volatility models. *Journal of Business & Economic Statistics*, 41(4):1215–1227, 2023. doi: 10.1080/07350015.2022.2116027.
- Donggyu Kim, Minseog Oh, Xinyu Song, and Yazhen Wang. Factor overnight GARCH-Itô models. *Journal of Financial Econometrics*, 22(5):1209–1235, 2024. doi: 10.1093/jjfinec/nbad032.
- Oliver Linton and Jianbin Wu. A coupled component DCS-EGARCH model for intraday and overnight volatility. *Journal of Econometrics*, 217(1):176–201, July 2020. doi: 10.1016/j.jeconom.2019.12.015.
- Larry J. Lockwood and Thomas H. McInish. Tests of stability for variances and means of overnight/intraday returns during bull and bear markets. *Journal of Banking & Finance*, 14(6):1243–1253, 1990.
- Dong Lou, Christopher Polk, and Spyros Skouras. A tug of war: Overnight versus intraday expected returns. *Journal of Financial Economics*, 134(1):192–213, October 2019. doi: 10.1016/j.jfineco.2019.03.011.
- Fariborz Moshirian, Huy G. L. Nguyen, and Peter K. Pham. Overnight public information, order placement, and price discovery during the pre-opening period. *Journal of Banking & Finance*, 36(10):2837–2851, 2012. doi: 10.1016/j.jbankfin.2012.06.007.
- Guilherme V. Moura, André A. P. Santos, and Esther Ruiz. Comparing high-dimensional conditional covariance matrices: Implications for portfolio selection. *Journal of Banking & Finance*, 118:105882, September 2020. doi: 10.1016/j.jbankfin.2020.105882.
- Dong Hwan Oh and Andrew J. Patton. Dynamic factor copula models with estimated cluster assignments. *Journal of Econometrics*, 237(2):105374, December 2023. doi: 10.1016/j.jeconom.2022.07.012.
- Marc S. Paolella, Paweł Polak, and Patrick S. Walker. A non-elliptical orthogonal garch model for portfolio selection under transaction costs. *Journal of Banking & Finance*, 125:106046, April 2021. doi: 10.1016/j.jbankfin.2021.106046.
- Efthymia Symitsi, Lazaros Symeonidis, Apostolos Kourtis, and Raphael Markellos. Covariance

forecasting in equity markets. *Journal of Banking & Finance*, 96:153–168, November 2018. doi: 10.1016/j.jbankfin.2018.08.013.

Chen Tong and Peter Reinhard Hansen. Characterizing correlation matrices that admit a clustered factor representation. *Economics Letters*, 233:111433, December 2023. doi: 10.1016/j.econlet.2023.111433.

Chen Tong and Peter Reinhard Hansen. Dynamic factor correlations. *Journal of Applied Econometrics*, 2026. ISSN 0883-7252 1099-1255. doi: 10.1002/jae.70062. Forthcoming.

Chen Tong, Peter Reinhard Hansen, and Ilya Archakov. Cluster GARCH. *Journal of Business & Economic Statistics*, 44(1):148–161, January 2026. doi: 10.1080/07350015.2025.2510325.

Y. K. Tse and Albert K. C. Tsui. A multivariate generalized autoregressive conditional heteroscedasticity model with time-varying correlations. *Journal of Business & Economic Statistics*, 20(3):351–362, 2002. doi: 10.1198/073500102288618496.